Earth and Planetary Science Letters 307 (2011) 501–516

Contents lists available at ScienceDirect

Earth and Planetary Science Letters

journal homepage: www.elsevier.com/locate/epsl

Differentiation of the continental crust by relamination

Bradley R. Hacker [a,*], Peter B. Kelemen [b], Mark D. Behn [c]

[a] Earth Science, University of California, Santa Barbara, California, USA
[b] Lamont Doherty Earth Observatory, Columbia University, Palisades, NY, USA
[c] Geology and Geophysics, Woods Hole Oceanographic Institution, Woods Hole, MA, USA

ARTICLE INFO

Article history:
Received 14 February 2011
Received in revised form 12 May 2011
Accepted 13 May 2011
Available online 2 June 2011

Editor: T.M. Harrison

Keywords:
continental crust
relamination
differentiation
subduction erosion
subduction
continental refinery

ABSTRACT

Crust extracted from the mantle in arcs is refined into continental crust in subduction zones. During sediment subduction, subduction erosion, arc subduction, and continent subduction, mafic rocks become eclogite and may sink into the mantle, whereas more silica-rich rocks are transformed into felsic gneisses that are less dense than peridotite but more dense than the upper crust. These more felsic rocks rise buoyantly, undergo decompression melting and melt extraction, and are relaminated to the base of the crust. As a result of this process, such felsic rocks could form much of the lower crust. The lower crust need not be mafic and the bulk continental crust may be more silica rich than generally considered.

1. Introduction: differentiation of the continental crust

The origin and composition of continental crust—particularly the lower crust—remain enigmatic. The principal conundrum to be resolved is how an andesitic to dacitic continental crust has formed when most mantle-derived magmas are basaltic. This differentiation has been explained as the result of lower crustal foundering (Arndt and Goldstein, 1989; Kay and Kay, 1991), crustal formation from primary mantle-derived andesitic magmas (Kelemen, 1995), or the mixing of basaltic rock with silicic magma derived by partial melting of mafic, subducting crust (Martin, 1986).

In their seminal papers, Herzberg et al. (1983) and Ringwood and Green (1966) introduced the idea that igneous processes can lead to crustal differentiation by lower crustal foundering if mantle-derived basaltic magma intruded into the crust forms a buoyant differentiate that is retained in the crust, plus a dense, olivine- and pyroxene-rich residue that sinks into the mantle (Fig. 1A). Kay and Kay (1991) expanded this idea by postulating that differentiation and lower crustal foundering might also be driven by the formation of metamorphic garnet in mafic rock (Fig. 1B). Jull and Kelemen (2001) quantified aspects of lower crustal foundering, and noted that buoyancy and viscosity requirements restrict significant lower crustal foundering to relatively warm environments such as rifts or active volcanoplutonic arcs. Though foundering of dense garnet granulites and pyroxenites probably is recorded in some arc sections (DeBari and Sleep, 1991; Kelemen et al., 2003a), loss of these rocks still yielded a mafic arc crust very different from continental crust (DeBari and Sleep, 1991; Greene et al., 2006). This is so because garnet-free mafic rocks that are either density-stable or too viscous to founder remain in the cold, upper and middle crust.

Whereas foundering of dense material could potentially produce a differentiated continental crust, two other tectonic processes—subduction erosion (Fig. 1C) and sediment subduction (Fig. 1D) (von Huene and Scholl, 1991)—are usually presumed to work in the opposite sense, by returning differentiated crust to the mantle. The most recent calculations (Scholl and von Huene, 2007) suggest that this process recycles continental crust back into the mantle at the same rate that continental crust is created. This could produce a steady-state crustal volume (Armstrong, 1981) and a constant composition.

This paper investigates another paradigm for differentiation of the continental crust: *The mantle produces differentiated crust in intra-oceanic arcs. This raw crustal material is subsequently subducted, devolatilized, and melted, and separated into a mafic residue that returns to the mantle and a felsic fraction that is relaminated to the base of the crust in the upper plate. This process will be most efficient in arcs where upper mantle temperatures are sufficiently high at the base of the crust* (Kelemen et al., 2003b) *to permit vertical viscous flow due to lithologic buoyancy of the felsic fraction* (Jull and Kelemen, 2001). This 'continental refinery' makes continental crust. We envision that this refining of raw crustal material into continental crust can take place via relamination during four subduction-zone processes (Fig. 2): i) sediment subduction, ii) arc subduction, iii) subduction erosion, and iv) continent subduction.

* Corresponding author.
E-mail address: hacker@geol.ucsb.edu (B.R. Hacker).

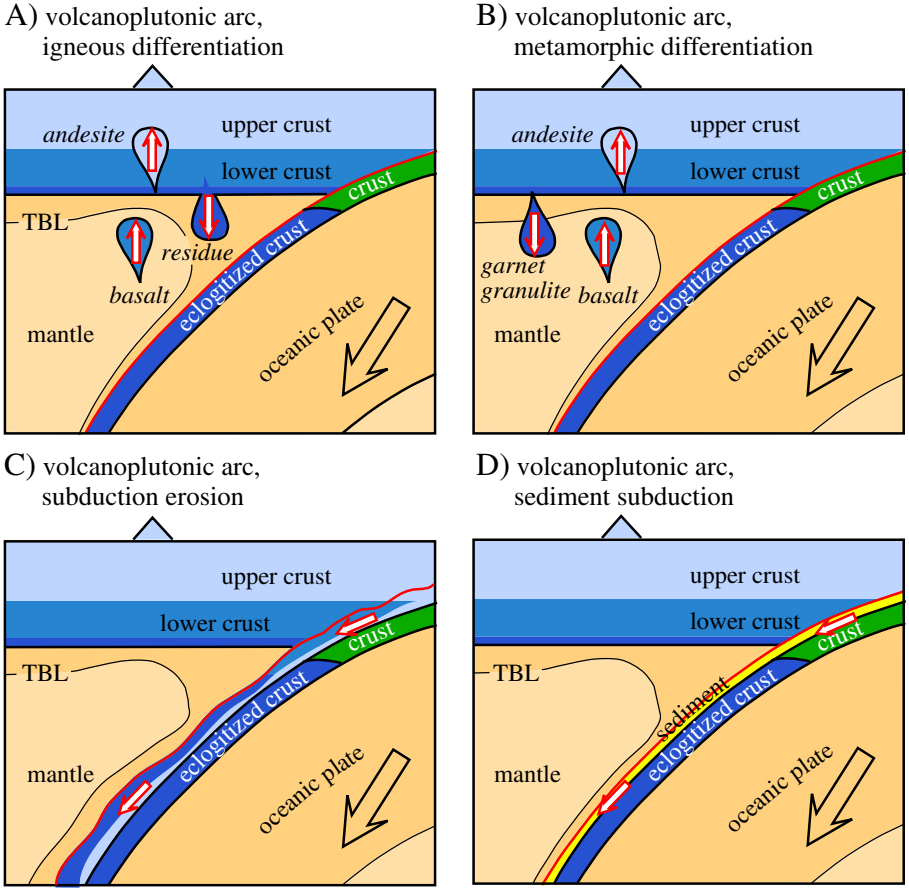

Fig. 1. Long-term change in the composition of the continental crust has conventionally been viewed as the result of two major "subduction factory" processes. A) Mantle-derived magma introduced into volcanoplutonic arcs differentiates into an andesitic fraction that is retained in the crust and an ultramafic cumulate that becomes part of the mantle (Arndt and Goldstein, 1989). B) Mafic rock at the base of a thick volcanoplutonic arc is converted into garnet granulite and sinks into the mantle (Herzberg et al., 1983). Two other major subduction-related processes are envisioned to work in the opposite sense, by removing differentiated material from the crust and returning it to the mantle. C) Crustal material ablated from the upper plate of a subduction system is returned to the mantle by subduction erosion (Scholl and von Huene, 2007; von Huene and Scholl, 1991). D) Trench sediments are returned to the mantle by subduction (Hilde, 1983). TBL: thermal boundary layer in mantle.

The relamination process can take the form of a) imbrication of material beneath the crust in the upper plate (Kimbrough and Grove, 2007), b) buoyant ascent from mantle depths to the base of the crust along a "subduction channel" (Gerya et al., 2007; Li and Gerya, 2009; Warren et al., 2008), and/or c) ascent of buoyant diapirs through the mantle wedge to the base of the crust (Behn et al., in review; Currie et al., 2007; Gerya and Meilick, 2011; Gerya and Yuen, 2003; Gorczyk et al., 2006; Kelemen et al., 2003a; Yin et al., 2007; Zhu et al., 2009). As discussed below, these processes may be more efficient than lower crustal foundering at generating large volumes of material with the major- and trace-element composition of continental crust, by relaminating the base of the crust with buoyant felsic rocks, and by purging the crust of eclogitized mafic rocks and dense residues produced by melting.

2. The composition and physical properties of continental crust

Earth's continental crust is distinct from the underlying mantle in that it is andesitic to dacitic (rather than ultramafic), has slower seismic velocities (V_P ~6–7 km/s, rather than >7.5 km/s) and is less dense (~2600–3000 kg/m^3, rather than >3300 kg/m^3) (Christensen and Mooney, 1995). It is typically subdivided into two or three discrete layers (Fig. 3A) on the basis of seismic velocities (Holbrook et al., 1992; Smithson, 1978), and considerable work has gone into inferring the compositions of these layers. Dividing the crust into three compositionally distinct layers on the basis of seismic velocity may be unwarranted because of the poor correlation between velocity and composition (Behn and Kelemen, 2003); the velocity of the lower crust could be higher than the mid crust due to mineralogical differences, such as the presence of garnet in the lower crust, rather than to a systematic compositional difference. Thus, here we make the simplifying assumption that there are just two layers: an upper crust and a lower crust (Fig. 3B).

The composition and physical properties of the upper continental crust are reasonably well known from exposures and from the composition of fine-grained clastic sediment such as shale and loess (e.g., the upper crust averages ~67 wt.% SiO_2; Rudnick and Gao, 2003). The composition of the lower crust, however, is more enigmatic. The principal difficulty is that, while there are many metamorphic terrains that record peak pressures of 8 to 12 kb, corresponding to lower crustal depths in cratons and mid-crustal levels of orogenic plateaus, there is no consensus that these are representative of typical or "average" lower crust. This problem applies to inferred "mid-crustal" exposures as well. Similarly, xenoliths erupted from lower crustal depths may be atypical because the basaltic lavas that host most xenoliths may not erupt through felsic lower crust (Jaupart and Mareschal, 2003) or may assimilate felsic xenoliths.

Physical properties (i.e., velocity, gravity, and heat flow) provide indirect constraints on the composition of the lower crust (Rudnick and Gao, 2003). For instance, the measured P-wave velocity of the lower crust is typically 6.7–7.1 km/s (Christensen and Mooney, 1995; Rudnick and Fountain, 1995), most likely corresponding to densities of 2900–3200 kg/m^3 (Christensen and Mooney, 1995). This has been

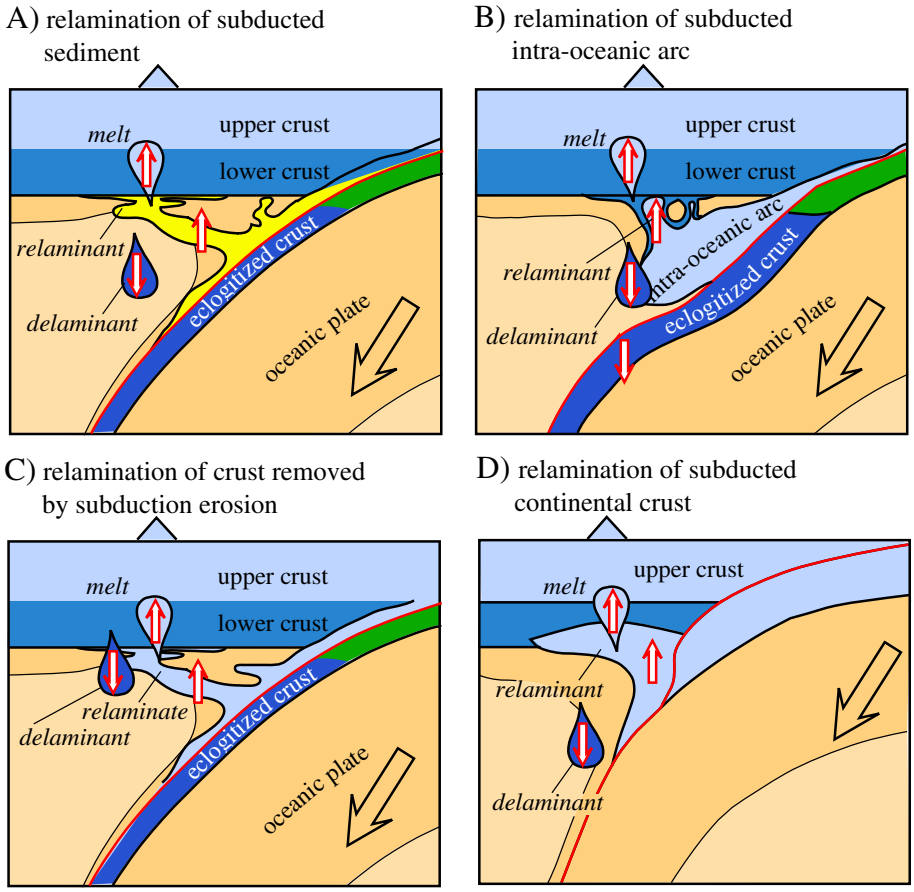

Fig. 2. Four tectonic settings for continental refining via relamination. In all cases, the relaminating layer may be thrust directly beneath existing crust, rise en bloc, perhaps in a "subduction channel", or rise as diapirs through the mantle wedge, depending on physical conditions. In all cases, there may be melting that produces a liquid that ascends well above the relaminating layer and residues that are either positively or negatively buoyant with respect to the adjacent mantle. 1) Subducted sediment is thrust into or beneath arc lower crust, or is gravitationally unstable and rises to relaminate the base of the crust in the upper plate. 2) Subducted volcanoplutonic arcs undergo density separation as the mafic lower crust transforms to eclogite while the buoyant upper crust relaminates the base of the crust in the upper plate. 3) Felsic crustal material removed from the upper plate by subduction erosion is relaminated to the base of the crust in the upper plate; mafic material transforms to eclogite and sinks within the upper mantle. 4) Subducted felsic continental crust is relaminated to the base of the crust in the upper plate. Any (ultra)mafic material of sufficient size transforms to eclogite and returns to upper mantle.

used to infer that the lower crust is mafic (Rudnick and Fountain, 1995), but this range of velocities can be satisfied by a wide variety of rocks that range from 50 to 65 wt.% SiO_2 and have similarly broad ranges of other major elements (Behn and Kelemen, 2003; Holbrook et al., 1992; Pakiser and Robinson, 1966; Reid et al., 1989; Rudnick and Fountain, 1995).

Heat-producing element abundances in the upper crust (producing 1.6 μW/m^3) and inferred mantle heat flow have been subtracted from measured surface heat flow (51 mW/m^2 in Paleozoic terrains, Jaupart and Mareschal, 2003) to infer that the lower crust is relatively unradiogenic (Rudnick and Fountain, 1995). For example, in Rudnick and Gao's (2003) model for a three-layer crust and a mantle heat flow of 17 mW/m^2, a 17-km thick lower crust can have a heat production rate of no more than 0.2 μW/m^3, implying that it contains less than 0.6 wt.% K_2O, 1.2 ppm Th and 0.2 ppm U (Fig. 3A) (Rudnick and Gao, 2003). Such a low inferred heat production rate, together with the compositions of post-Archean crustal xenoliths assumed to be representative of the lower crust, leads to the conclusion that the lower crust is dominantly (80%) mafic rock with, e.g., 53.4 wt.% SiO_2 (Rudnick and Gao, 2003). If true, the principal tectonic process responsible for producing the lower crust might be underplating of mantle-generated, mafic melts or the accumulation of refractory products of fractional crystallization or anatexis.

However, neither mantle heat flow nor the distribution of radiogenic elements in the crust are well known. If either mantle heat flow or the concentration of radiogenic elements in the "mid-crust" has been overestimated, the radiogenic element concentration in the lower crust could be substantially higher, and thus the lower crust could contain a higher proportion of felsic rocks. As an extreme example, using the lower bound on mantle heat flow through Precambrian terrains of 11 mW/m^2 (Jaupart and Mareschal, 2003) and assuming that there is no compositional distinction between the "mid-crust" and the lower crust, a surface heat flow of 51 mW/m^2 allows a 26-km thick middle + lower crust composed of typical 'post-Archean' lower crustal granulites (Rudnick and Presper, 1990 database updated to 2003), with a median of 64 wt.% SiO_2 and a median heat-production rate of 0.7 μW/m^3 (Fig. 3B). In this case, no mafic lower crust is required by the seismic data or by the heat-flow data, and much of the lower crust could be felsic (Table 1).

Other data support the possibility that a significant proportion of the lower crust is composed of felsic, metasedimentary rocks. A minimum estimate for the proportion of metasediments in the lower continental crust can be derived using (Nesbitt and Young's (1984) algorithm for identifying peraluminous compositions (an excess of Al_2O_3 relative to alkali elements, which stabilizes minerals more aluminous than plagioclase—a characteristic of metasediments). This methodology reveals that more than 27% of samples from granulite terrains, more than 14% of granulite xenoliths, and more than 43% of rocks from ultrahigh-pressure terrains (see below)—but only ~6% of Archean granulites—are peraluminous, pelitic metasediments (Fig. 4). These are minimum estimates of the proportion of felsic metasediments in the lower crust because metamorphosed

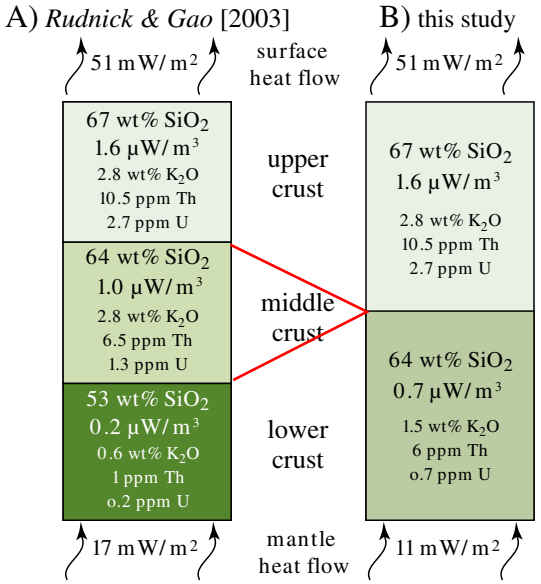

Fig. 3. (A) The Rudnick and Gao (2003) three-layer model for the crust, which uses a mantle heat flow of 17 mW/m^2, the measured composition of the upper crust, an inferred middle crust composition, lower crustal wavespeeds, and the compositions of xenoliths to conclude that the lower crust is relatively unradiogenic. Alternatively, (B) using a lower, 11 mW/m^2, bound (Jaupart and Mareschal, 2003) on mantle heat flow and assuming a two-layer crust, we find that the lower crust may be more felsic and three times more radiogenic than estimated by Rudnick and Gao (2003).

immature quartzofeldspathic sediment ("wacke") is not peraluminous, and has an Al_2O_3/alkali ratio indistinguishable from metaluminous igneous rocks.

Thus, geophysical constraints permit the lower crust to be quite felsic and radiogenic—including significant amounts of peraluminous sediments—and the tectonic processes responsible for producing the lower crust may be different than commonly assumed.

3. Effects of prograde metamorphism and melting on rock physical properties

Before describing the relamination model, we review how the physical properties of crustal rocks—including density and seismic velocity—change in response to prograde metamorphism, partial melting, and melt extraction. Consider four compositions that span the range of crustal rock types: pelite (metamorphosed mudrock), wacke (immature quartzofeldspathic sediment), tonalite, and a mid-ocean ridge basalt (MORB) (Table 2). Because of the paucity of melt activity models for the conditions of interest, the effects of partial melting are best seen in experimental studies (Table 3) that i) used compositions similar to typical pelite, wacke, tonalite, and MORB, and that ii) reported phase proportions and compositions (Auzanneau et al., 2006; Montel and Vielzeuf, 1997; Patiño Douce, 2005; Patiño Douce and Harris, 1998; Rapp and Watson, 1991; Rapp and Watson, 1995; Schmidt et al., 2004; Sen and Dunn, 1994; Singh and Johannes, 1996; Vielzeuf and Holloway, 1988; Vielzeuf and Montel, 1994; Wolf and Wyllie, 1993). Fig. 5 shows the results of these studies: the amount of melt (Fig. 5A), the SiO_2 content of the melt (Fig. 5B), the K_2O content of the melt (Fig. 5C). It also shows the P-wave velocity (Fig. 5D) and density (Fig. 5E) calculated with the method of Hacker and Abers (2004), using the composition of the residue calculated from the modes and compositions of the solid phases in the experiments.

To quantify the effects of subsolidus prograde metamorphism, we calculated phase proportions and compositions for the same experimental bulk compositions using Perple_X v. 7 (Connolly, 1990) and the 2004 Holland and Powell (Holland and Powell, 1998) database; for similar, recent approaches using other bulk compositions, see Massonne et al. (2007) and Semprich et al. (2010). We used the following solution models: amphibole (Wei and Powell, 2003; White et al., 2003), biotite (Powell and Holland, 1999), chlorite (Holland et al., 1998), clinopyroxene (Holland and Powell, 1996), K-feldspar (Thompson and Hovis, 1979), K-white mica (parameters from Thermocalc), garnet (Holland and Powell, 1996), and plagioclase (Fuhrman and Lindsley, 1988). We then calculated rock physical properties via the method of Hacker and Abers (2004). We used the same bulk H_2O contents as the experimental melting studies and removed from the bulk composition any H_2O produced by dehydration along prograde P–T paths. This minimizes the effects of dehydration and melting on changes in the rock physical properties. H_2O-present melting is thus not considered.

We focus on two endmember PT paths (Fig. 6A) for the continental refinery model. These paths involve compression to 3 GPa and heating to 800 °C or 1050 °C, followed by decompression and cooling to 700 °C and 1 GPa. The first path is meant to simulate slab-top conditions in a

Table 1
Composition of Earth's crust.

	Rudnick and Gao, 2003		This study	
	Entire crust	Lower crust	Entire crust*	Middle and lower crust‡
SiO_2	60.6	53.4	65.2	64.4
TiO_2	0.72	0.8	0.7	0.7
Al_2O_3	15.9	16.9	15.0	14.8
FeOT	6.71	8.6	5.8	6.1
MnO	0.1	0.1	0.1	0.1
MgO	4.66	7.2	2.5	2.5
CaO	6.41	9.6	3.4	3.4
Na_2O	3.07	2.7	3.0	2.8
K_2O	1.81	0.6	1.9	1.5
P_2O_5	0.13	0.1	0.1	0.1
Total	100.12	100.0	99.9	99.8
Mg#	55.3	60.1	44.0	42.5
Li	16	13	13	7
Sc	21.9	31.0	19.0	21.8
V	138	196	89	84
Cr	135	215	65	51
Co	26.6	38.0	21.3	23.5
Ni	59	88	31	22
Cu	27	26	19	14
Zn	72	78	69	71
Ga	16	13	18	19
Rb	49	11	55	41
Sr	320	348	246	206
Y	19	16	24	25
Zr	132	68	169	156
Nb	8	5	11	10
Cs	2	0	2	0
Ba	456	259	473	390
La	20	8	23	19
Ce	43	20	56	53
Pr	4.9	2	8	8
Nd	20	11	26	26
Sm	3.9	2.8	5.1	5.4
Eu	1.1	1.1	1.4	1.6
Gd	3.7	3.1	4.4	4.6
Tb	0.6	0.5	0.8	0.8
Dy	3.6	3.1	3.5	3.4
Ho	0.77	0.68	0.73	0.68
Er	2.1	1.9	2.1	2.0
Yb	1.9	1.5	2.3	2.5
Lu	0.3	0.3	0.4	0.5
Hf	3.7	1.9	4.0	3.3
Ta	0.7	0.6	0.6	0.4
Pb	11	4	15	14
Th	5.6	1.2	7.3	5.6
U	1.3	0.2	1.4	0.7

*The composition of the crust is constructed using 14 km of the upper crustal composition of Rudnick and Gao (2003), plus 26 km of the median values for post-Archean granulite terrains(‡) from the updated Rudnick and Presper (1990) database. (See Fig. 3.)

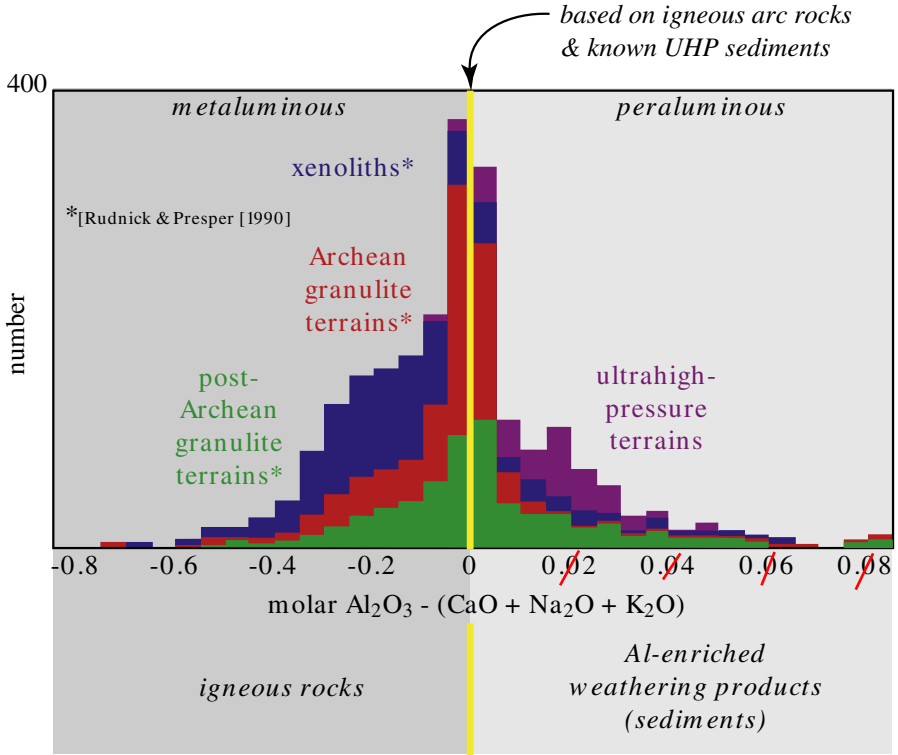

Fig. 4. A significant fraction of ultrahigh-pressure rocks, lower crustal xenoliths, and lower crustal terrains are peraluminous, pelitic metasediments. Many other quartzofeldspathic rocks in these suites could be metaluminous metasediments that are compositionally indistinguishable from igneous rocks.

warm subduction zone (Syracuse et al., 2010) and the second simulates more extreme P–T conditions recorded by some UHP terrains and xenoliths (see below). The end of the paths at 700 °C and 1 GPa simulate relamination to the continental Moho in a convergent orogen; we consider i) complete mineralogical re-equilibration at 700 °C and 1 GPa (but no change in H_2O content),and ii) metastable preservation of the high-pressure mineralogy, except for coesite, which we assumes converts back to quartz.

For the modeled PT paths, the *pelite* undergoes large subsolidus increases in density and velocity (solid line in Fig. 6B) largely due to the growth of garnet; there is a particularly large—but reversible—increase associated with the quartz–coesite transformation. For the cold path, the pelite reaches a maximum density of ~3200 kg/m^3 (unfilled diamond in Fig. 6B). Subsequent re-equilibration at Moho conditions returns the rock to nearly its original physical properties (open square in Fig. 6B); if the pelite reaches the Moho, but retains its

Table 2
Bulk compositions (wt.%) of typical crustal rocks and Talkeetna arc harzburgite.

	SiO_2	TiO_2	Al_2O_3	FeO + MnO	MgO	CaO	Na_2O	K_2O	H_2O
Pelite									
[Shaw, 1956]	61.5	0.8	17.0	6.3	2.5	1.8	1.8	3.5	3.5
[Ferry, 1982]	60.8	0.8	16.9	7.1	3.4	1.2	1.7	3.7	1.4
Used in Perple_X (after Vielzeuf and Holloway, 1988, and other studies)	64.4	0.8	18.1	6.4	2.4	1.5	1.7	2.6	2.1
Wacke									
[Pettijohn, 1963]	66.7	n.d.	13.5	4.9	2.1	2.5	2.9	2.0	n.d.
[Whetten et al., 1969]	66.5	n.d.	13.9	4.2	2.0	3.4	2.9	2.1	n.d.
[Ernst et al., 1980]	66.1	0.6	13.2	5.0	3.9	2.1	3.2	1.8	n.d.
Used in Perple_X (after Montel and Vielzeuf, 1997, and other studies)	70.4	0.7	13.1	4.9	2.4	1.7	3.0	2.4	1.5
Tonalite									
[Nockolds, 1954]	66.2	0.6	15.6	4.7	1.9	4.7	3.9	1.4	0.0
[Rollinson and Windley, 1980]	62.3	0.6	16.1	5.9	2.8	6.7	4.4	0.7	n.d.
[Sheraton and Collerson, 1983]	69.8	0.4	14.5	3.5	1.3	4.0	4.4	0.8n.d.	
[Schmidt, 1993]	59.0	0.7	16.8	6.0	3.2	6.5	2.8	2.4	1.1
http://www.earthchemportal.org/used in Perple_X (after Patiño Douce, 2005)	63.9	0.6	16.1	5.1	2.4	5.1	3.7	1.9	0.0
	60.8	0.9	16.9	6.0	2.7	6.3	3.8	2.5	0.7
MORB									
[Pearce, 1976], used in Perple_X	50.6	1.5	15.7	10.6	7.6	11.1	2.6	0.2	1.6
Talkeetna Arc harzburgite									
P.B. Kelemen unpublished XRF data normalized to 100%	44.6	0.0	0.6	8.0	46.0	0.5	0.0	0.0	n.d.

Table 3
Reported melt compositions, normalized to 100% anhydrous, and calculated residue compositions.

T °C	P GPa	%melt	SiO_2	TiO_2	AL_2O_2	FEO	MnO	MgO	CAO	NA_2O	K_2O	H_2O	SiO_2	TiO_2	AL_2O_3	FEO	MnO	MgO	CaO	Na_2O	K_2O	H_2O
Vielzeuf and Holloway (1988) pelite																						
SM			65.8	0.8	18.5	6.4	0.1	2.5	1.6	1.7	2.6	2.2										
875	1	57	73.1	0.3	16.1	1.5	0.1	1.0	0.4	3.1	4.4	3.7	62.9	0.0	22.6	8.9	0.0	2.0	2.0	1.4	0.1	0.0
900	1	62	71.2	0.6	16.1	1.9	0.1	1.3	1.6	3.0	4.2	3.5	55.3	0.0	21.1	16.5	0.0	4.1	3.0	0.0	0.0	0.0
950	1	64	69.4	0.6	17.0	2.9	0.1	1.2	1.8	2.8	4.2	3.4	55.2	0.0	21.5	16.5	0.2	3.9	2.8	0.0	0.0	0.0
1000	1	63	69.2	0.6	17.2	2.4	0.1	1.6	1.7	3.5	3.7	3.4	59.6	0.0	21.3	12.2	0.2	6.1	0.5	0.0	0.0	0.0
1050	1	75	66.1	1.0	17.6	5.1	0.1	2.0	1.7	2.8	3.7	2.8	57.3	0.0	21.9	13.3	0.2	6.7	0.6	0.0	0.0	0.0
1100	1	72	65.4	1.1	17.6	5.5	0.1	2.1	1.9	2.7	3.6	3.0	58.8	0.0	22.0	12.1	0.2	6.3	0.5	0.0	0.0	0.0
1150	1	81	65.5	0.9	17.5	6.5	0.1	2.2	1.7	2.6	3.1	2.6	63.7	0.0	24.5	6.6	0.0	5.0	0.1	0.0	0.0	0.0
1200	1	92	64.6	1.0	18.1	6.8	0.1	2.5	1.6	2.2	3.1	2.3	75.5	0.0	24.5	0.0	0.0	0.0	0.0	0.0	0.0	0.0
Schmidt et al. (2004) pelite																						
SM			65.8	0.8	18.5	6.4	0.1	2.5	1.6	1.7	2.6	2.2										
850	4	8	76.8	0.3	13.4	0.8	0.0	0.3	0.9	2.4	5.1	15.0	64.6	0.9	18.9	6.9	0.1	2.7	1.6	1.5	2.0	0.9
900	4	19	76.6	0.4	13.4	0.8	0.0	0.2	0.7	2.4	5.6	11.0	63.5	1.0	19.8	7.7	0.1	3.0	1.8	1.1	1.3	0.6
950	4	20	75.0	0.9	13.6	1.1	0.0	0.2	0.9	2.7	5.6	11.0	63.6	0.8	19.8	7.7	0.1	3.1	1.7	1.0	1.5	0.7
1000	4	49	71.4	1.2	14.7	2.0	0.0	0.6	1.4	3.5	5.3	4.3	60.4	0.5	22.3	10.6	0.2	4.3	1.7	0.0	0.0	0.0
950	5	42	72.0	0.4	15.0	1.1	0.0	0.3	0.9	4.0	6.3	5.1	61.2	1.2	21.1	10.2	0.2	4.1	2.0	0.0	0.0	0.0
1000	5	44	71.6	0.5	15.3	1.3	0.0	0.3	0.9	3.9	6.2	5.0	61.1	1.1	21.0	10.4	0.2	4.2	2.0	0.0	0.0	0.0
Montel and Vielzeuf (1997) wacke																						
SM			71.5	0.7	13.3	4.9	0.1	2.4	1.7	3.0	2.5	1.3										
803	1	14	74.1	0.2	16.0	0.9	0.0	0.4	0.6	3.5	4.2	3.7	70.4	0.8	12.1	5.8	0.0	2.8	1.4	3.0	2.7	1.1
858	1	31	73.2	0.1	16.1	1.0	0.2	0.4	0.8	3.4	4.8	8.8	70.9	2.0	12.6	4.1	0.3	2.8	1.4	2.8	2.3	0.8
860	1	23	72.5	0.3	16.2	1.3	0.1	0.6	0.7	3.5	4.8	4.0	69.8	0.6	12.7	3.7	3.0	2.7	1.6	2.9	2.1	0.8
885	1	17	71.1	0.4	16.0	1.9	0.0	0.5	0.8	3.7	5.5	4.1	71.1	0.6	13.3	4.7	0.0	2.0	2.5	3.1	1.8	0.8
1000	1	36	71.3	0.5	15.8	2.1	0.0	0.6	0.6	3.3	5.8	4.5	72.6	1.9	12.3	6.3	0.1	1.0	2.1	1.0	2.7	0.0
1000	1	36	71.1	0.4	16.0	1.9	0.0	0.5	0.8	3.7	5.5	4.1	73.6	1.5	12.6	5.4	0.1	0.5	2.3	1.1	2.9	0.0
Auzanneau et al. (2006) wacke																						
SM			71.5	0.7	13.3	4.9	0.1	2.4	1.7	3.0	2.5	1.3										
900	2.2	42	72.2	0.3	16.0	0.5	0.0	0.2	0.8	5.5	4.4	3.0	69.7	0.9	12.7	5.9	0.1	2.9	2.0	2.6	2.2	1.2
900	2.2	39	72.1	0.2	16.1	0.5	0.0	0.3	1.0	5.3	4.5	3.2	70.7	0.8	11.2	8.1	0.2	4.0	2.4	1.2	1.1	0.5
850	2.3	27	72.7	0.2	15.7	0.6	0.0	0.3	0.5	5.4	4.5	3.6	70.3	0.9	12.2	6.5	0.2	3.2	2.1	2.1	1.7	0.9
870	2.4	27	73.2	0.2	15.7	0.5	0.1	0.2	0.3	5.2	4.6	3.2	70.1	0.7	12.0	7.1	0.1	3.2	2.5	2.3	1.4	0.6
Schmidt et al. (2004) wacke																						
SM			71.5	0.7	13.3	4.9	0.1	2.4	1.7	3.0	2.5	1.3										
900	4	18	75.2	0.4	13.5	0.8	0.0	0.3	0.6	2.3	6.9	8.4	71.1	0.8	13.3	5.9	0.1	2.9	2.0	2.5	1.0	0.5
950	4	18	73.6	0.6	14.3	0.9	0.0	0.4	0.9	3.2	6.1	8.2	71.5	0.7	13.1	5.8	0.1	2.9	1.9	2.3	1.1	0.5
1000	4	58	70.4	1.0	15.6	1.6	0.0	0.8	1.4	5.1	4.1	2.6	73.1	0.3	10.2	9.5	0.1	4.6	2.1	0	0.0	0.0
900	5	9	74.0	0.4	13.0	1.2	0.1	0.2	0.3	3.1	7.7	8.0	72.9	0.8	13.6	5.4	0.1	2.7	1.9	2.7	0.0	0.0
950	5	32	71.0	0.3	15.6	0.9	0.1	0.3	0.5	3.5	7.9	4.6	72.3	0.9	12.3	6.9	0.1	3.4	2.3	1.9	0.0	0.0
1000	5	41	71.9	0.6	15.8	1.1	0.0	0.3	0.6	3.7	6.1	3.5	71.8	0.8	11.6	7.7	0.1	3.9	2.5	1.6	0.0	0.0
Patiño Douce (2005) tonalite																						
SM			60.9	0.9	16.9	5.9	0.1	2.7	6.3	3.8	2.5	0.7										
950	1.5	18	73.2	0.3	15.0	0.9	0.0	0.3	1.1	4.7	4.5	5.1	59.8	0.5	17.8	7.1	0.2	3.2	6.4	2.7	2.2	0.1
940	2.1	10	73.0	0.2	15.7	0.5	0.0	0.3	0.9	5.5	3.8	9.8	62.6	0.4	14.6	6.3	0.2	3.9	5.7	2.6	3.7	0.0
960	2.1	12	72.7	0.3	15.6	0.8	0.0	0.3	1.2	5.3	3.9	8.1	58.6	1.0	17.1	6.8	0.1	3.1	7.3	3.6	2.3	0.0
975	2.1	16	72.6	0.2	15.9	0.7	0.1	0.2	1.1	5.2	4.0	6.3	58.4	0.5	17.1	7.4	0.2	4.9	6.2	2.4	2.9	0.0
1025	2.1	33	72.9	0.4	15.3	1.2	0.0	0.2	0.9	5.0	4.1	3.1	53.7	0.6	19.8	9.0	0.2	5.0	8.9	2.6	0.1	0.0
1060	2.1	55	71.3	0.5	16.1	0.7	0.1	0.4	1.5	4.1	5.4	1.8	58.6	0.9	12.6	11.2	0.3	7.4	8.1	0.9	0.0	0.0
1025	2.7	8	73.4	0.1	15.6	0.4	0.0	0.0	0.8	2.8	6.9	8.5	62.0	0.2	19.9	5.5	0.1	1.2	4.7	3.4	2.6	0.4
1075	2.7	22	74.9	0.1	16.4	0.4	0.0	0.0	1.0	3.0	4.1	3.8	58.5	0.6	17.8	6.7	0.2	3.7	6.8	3.4	2.2	0.2
1100	2.7	26	73.8	0.3	16.6	0.8	0.0	0.1	1.1	3.0	4.3	3.5	56.1	0.9	18.9	7.3	0.1	3.9	7.3	3.4	1.8	0.1
1125	2.7	39	71.5	0.5	16.3	0.8	0.0	0.2	1.6	3.9	5.2	2.5	54.6	0.9	18.7	8.7	0.2	5.2	7.4	3.2	1.0	0.0
1150	2.7	45	70.6	0.6	16.5	1.0	0.0	0.3	1.8	3.9	5.3	2.2	55.1	0.9	18.8	9.6	0.3	5.3	7.9	2.0	0.0	0.0
975	3	9	75.5	0.2	16.6	0.5	0.0	0.1	1.0	2.1	4.0	7.3	57.9	0.3	18.9	6.3	0.2	2.5	7.4	3.7	2.3	0.5
1010	3	26	73.5	0.2	15.4	0.7	0.0	0.1	0.8	3.1	6.2	2.9	55.5	0.5	19.8	7.1	0.2	2.7	8.2	4.1	1.6	0.4
1075	3	45	72.2	0.4	16.1	0.7	0.0	0.1	0.9	3.6	6.1	2.1	53.2	0.7	17.1	9.8	0.2	5.8	9.0	3.8	0.2	0.1
1000	3.2	5	70.8	0.1	16.4	0.5	0.1	0.1	1.6	4.2	6.3	5.8	60.7	0.5	18.7	6.0	0.1	1.8	6.1	3.1	1.9	1.0
1050	3.2	31	73.3	0.2	16.1	0.6	0.1	0.1	0.9	3.9	4.8	2.5	56.6	0.5	19.1	8.4	0.2	3.1	7.1	3.9	0.7	0.4
1100	3.2	50	70.1	0.5	16.4	1.3	0.0	0.3	2.0	4.2	5.1	2.0	53.9	0.7	17.6	10.8	0.3	3.2	9.4	4.2	0.0	0.0
Rapp and Watson (1995) ophiolite pillow																						
SM			52.4	1.2	17.0	11.6	0.2	6.7	5.6	4.4	0.8	1.5										
1100	3.2	32	65.9	1.3	17.6	3.2	0.1	1.0	1.5	6.7	2.6		45.4	1.1	17.9	14.8	0.6	9.5	7.9	2.9	0.0	0.0
Rapp and Watson (1995) amphibolite Vermont																						
SM			49.7	2.1	17.4	10.9	0.2	6.2	9.9	3.4	0.2	0.7										
1100	3.2	22	65.1	2.21	15.7	4.62	0.09	1.51	4.42	5.72	0.7		43.6	1.7	18.2	15.4	0.3	7.5	10.9	2.3	0.1	0.0
Rapp and Watson (1995) ocean tholeiite																						
SM			49.0	0.7	15.5	10.8	0.2	8.5	12.8	2.3	0.1	1.0										
1050	2.2	26	66.4	0.8	17.9	3.3	0.0	1.1	4.5	5.5	0.5		44.5	0.9	15.6	13.8	0.3	10.5	13.5	1.2	0.0	0.0

Table 3 (*continued*)

T °C	P GPa	%melt	SIO_2	TIO_2	AL_2O_2	FEO	MnO	MgO	CAO	NA_2O	K_2O	H_2O	SIO_2	TIO_2	AL_2O_3	FEO	MnO	MgO	CaO	Na_2O	K_2O	H_2O
Rapp and Watson (1995) Archean pillow																						
SM			48.8	1.2	14.5	14.1	0.2	7.0	11.3	2.6	0.2	1.6										
1025	1.6	24	67.2	1.0	16.3	4.1	0.1	1.0	4.8	4.9	0.6		42.8	1.4	15.3	16.3	0.3	9.3	14.0	0.6	0.1	0.0
1050	1.6	27	61.7	1.25	17.6	6.21	0.11	1.48	6.31	4.9	0.5		43.2	0.9	16.6	15.7	0.3	9.7	13.0	0.5	0.1	0.0
Sen and Dunn (1994) amphibolite																						
SM			47.1	1.2	15.1	13.2	0.3	8.3	11.4	2.5	0.8	1.5										
925	1.5	2	69.5	0.26	16.7	1.35	0	0.35	1.5	4.5	5.9		46.5	1.1	14.6	12.8	0.2	8.7	11.7	2.0	0.6	1.7
950	1.5	15	70.1	0.54	16.1	2.4	0	0.69	2.5	4.6	3.1		45.2	1.1	16.2	13.7	0.2	8.4	11.2	2.0	0.5	1.4
950	1.5	9	67.6	0.63	17.6	2.4	0	0.74	2.4	5.6	3.1		45.2	1.2	15.3	12.6	0.1	9.2	12.3	2.1	0.5	1.5
950	1.5	9	66.4	0.6	18	3.1	0	0.85	3.4	5.2	2.5		45.6	1.2	14.8	12.7	0.2	9.1	12.0	2.2	0.6	1.6
975	1.5	19	68	0.7	17.1	2.99	0	0.92	2.9	4.64	2.8		44.2	1.3	15.4	14.9	0.3	9.2	11.4	1.7	0.4	1.3
975	1.5	12	65.3	0.76	18.5	2.85	0	0.72	2.6	6.5	2.7		45.4	1.5	14.9	13.8	0.2	9.0	12.8	2.0	0.1	0.3
1025	1.5	23	61.7	1.05	19	4.75	0	1.16	3.1	6.5	2.8		44.5	1.3	13.8	14.7	0.3	10.2	13.9	1.0	0.1	0.2
1025	1.5	20	62.8	1.06	18.4	4.8	0	1.29	3.5	5.5	2.6		44.0	1.3	15.0	14.0	0.2	9.9	13.4	1.4	0.2	0.6
900	2	23	71.3	0.3	16	1.2	0	0.36	1	4.7	5.2		45.4	1.5	14.9	13.8	0.2	9.0	12.8	2.0	0.1	0.3
950	2	15	67.6	0.6	17.5	1.9	0	0.62	1.6	4.89	5.3		46.0	1.2	14.9	13.3	0.2	9.4	13.0	1.9	0.0	0.0
975	2	16	66.1	0.8	17.8	2.5	0	0.68	1.9	5.7	4.5		45.5	1.2	15.0	13.3	0.2	10.1	13.2	1.5	0.0	0.0
1025	2	21	62	1.5	18.3	4.4	0	1.2	2.8	6.14	3.7		45.0	1.3	14.6	14.2	0.2	9.7	13.5	1.4	0.0	0.0
1150	2	25	56.4	2.3	17.6	7.6	0	2.1	5.6	5.9	2.5		44.8	0.9	15.4	13.8	0.2	10.6	13.4	1.0	0.0	0.0
Schmidt et al. (2004) *MORB*																						
SM			52.5	2.1	15.1	9.7	0.0	7.2	9.5	3.0	0.9	1.8										
850	4	14	73.0	0.4	13.7	1.0	0.0	1.1	2.3	2.8	5.7	12.5	49.2	2.3	15.4	11.1	0.0	8.2	10.6	3.0	0.1	0.1
900	4	15	73.4	0.3	13.7	0.9	0.0	1.0	2.1	2.8	5.9	12.2	48.8	2.4	15.4	11.2	0.0	8.3	10.8	3.0	0.1	0.0
950	4	16	73.1	0.6	14.1	1.2	0.0	0.9	2.1	2.8	5.3	11.0	48.6	2.3	15.3	11.3	0.0	8.4	10.9	3.0	0.1	0.0
1000	4	29	69.5	2.9	15.3	2.5	0.0	0.5	2.5	3.3	3.5	6.3	45.5	1.7	15.1	12.6	0.0	9.9	12.3	2.9	0.0	0.0

SM, starting material.

higher pressure mineralogy, its density and velocity undergo smaller reductions to ~3050 kg/m^3 and 6.5 km/s (filled square in Fig. 6B). On the hot path, melting due to phengite breakdown begins at 800–900 °C and produces 19% melt by 900 °C and 49% melt by 1000 °C (Fig. 5A; Table 3). Numerous experimental, theoretical, and field studies suggest that melt in volumes >10% can separate from its source under typical lower crustal conditions and migrate to shallower crustal levels (e.g., Brown, 2007). If the pelite melt does separate from the rock, the residue produced at 900 °C reaches densities >3300 kg/m^3, and at 1000 °C reaches densities >3500 kg/m^3 (Fig. 5E, unfilled diamonds in Fig. 6C). If the 900 °C residue subsequently becomes relaminated at the Moho, it attains a velocity and density typical of the lower crust, regardless of whether it re-equilibrates (unfilled square in Fig. 6C) or retains a metastable high-pressure mineralogy (filled square in Fig. 6C). A residue produced at 1000 °C will be negatively buoyant with respect to the mantle.

Along the same PT paths the *wacke* also undergoes subsolidus increases in density and velocity due to similar reactions and melt extraction. For the cold path, the wacke reaches a maximum density of >3100 kg/m^3; upon return to the Moho, the wacke returns to its original physical properties if equilibrium obtains (unfilled square in Fig. 6B), but stays at >2900 kg/m^3 if high-pressure phases are retained (filled square). On the hot path, melting due to phengite breakdown begins between 800 and 900 °C and the melt fractions are 18 and 58 vol% at 900 and 1000 °C, respectively (Table 3); if the melt separates from the rock at these temperatures, the residue reaches a density >3250 and >3350 kg/m^3. A residue produced at >1000 °C will be negatively buoyant with respect to the mantle. If returned to the Moho the residue densities and velocities are typical of the lower crust, regardless of whether the high pressure phases are retained.

Along the cold path, *tonalite* reaches a density of >3200 kg/m^3 due to the growth of garnet and clinopyroxene. Assuming equilibrium, decompression to 700 °C and 1 GPa produces a nearly complete reversion back to the initial density of ~2800 kg/m^3; if high pressure phases are retained, the density remains >3100 kg/m^3. Along the hot path, biotite-dehydration melting begins at ~900 °C and is finished by 1000 °C, producing ~25 vol% melt. If the melt separates, the residue produced at 975 °C reaches densities >3300 kg/m^3 at peak conditions. Decompression to 700 °C and 1 GPa under equilibrium conditions yields a density of ~3000 kg/m^3, typical of the lower crust (Fig. 6B), whereas metastable retention of high-pressure minerals leads to minimal reductions in physical properties. At temperatures of 1050 °C and higher, the residue is negatively buoyant with respect to the mantle.

By the time *MORB* with a normal K_2O content (0.2 wt.%) reaches 800 °C and 3 GPa, it has undergone significant dehydration due to the breakdown of amphibole, and is nearly anhydrous; the concomitant growth of garnet and omphacite leads to eclogite with a density >3400 kg/m^3. In such a dehydrated state, mafic rock will produce much less than the 10 vol% melt seen in experiments on H_2O-rich amphibolite (Fig. 5); extraction of such small amounts of melt would not cause significant changes in the physical properties of the residue compared to the protolith. Because this lithology is denser than the surrounding mantle, it is unlikely to ascend buoyantly unless surrounded by other less dense material. However, if it did, cooling to 1 GPa and 700 °C leads to a rock with a density >3200 kg/m^3. Along the hot PT path, melting begins at <900 °C and the volume of melt reaches 20–30% by 1050 °C in a MORB with 0.9 wt.% K_2O (Schmidt et al., 2004); if the melt separates, the residue reaches densities of ~3500 kg/m^3 (Fig. 6B). Unaltered MORB, with ~4× less K_2O will produce ~4× less melt, which will likely not separate from the residue. In the unlikely event that dry MORB eclogite returned to the base of the crust, it would have a 1 GPa, 700 °C density of ~3200 kg/m^3.

Thus, pelite, wacke and tonalite that undergo prograde metamorphism to 800 °C and 3 GPa (unfilled diamonds in Fig. 6) have densities comparable to or greater than the lower crust, but remain buoyant with respect to the mantle. In this case, they may rise to the Moho (700 °C and 1 GPa); if the high-pressure minerals remain metastable, these rocks have densities similar to the lower crust, whereas if the rocks convert to minerals stable at 1 GPa, they will have densities little different than at STP and could rise higher in the crust. At the same peak conditions, MORB undergoes significant dehydration and reaches densities greater than that of mantle peridotite regardless of whether it melts. Such eclogites may therefore sink into the mantle. If eclogite-facies MORB rises to the Moho, for example as small bodies entrained in buoyant felsic rocks as observed in UHP terrains, it will be markedly denser than at STP because of this dehydration, but will be gravitationally stable compared to the underlying mantle.

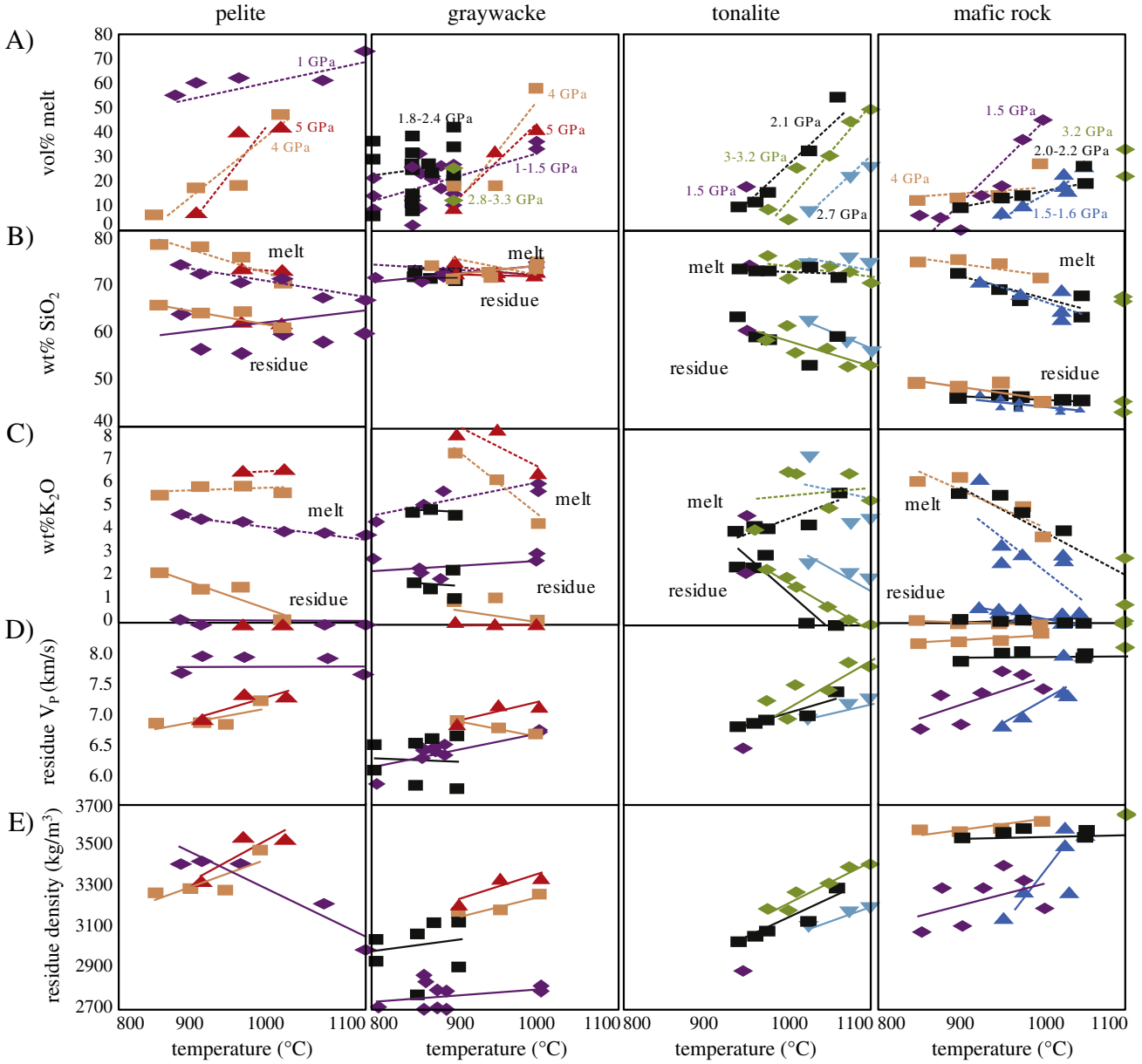

Fig. 5. Summary of dehydration-melting experiments on pelite, wacke, tonalite, and mafic rock. A) Reported vol% of melt. Pelite generates >50% melt at 1050 °C, wacke 30–40%, tonalite ~30%, and K-MORB or amphibolite generate ~20% at 1050 °C. The experiments on mafic rocks are not necessarily directly applicable to the conditions of interest in this paper, in that the starting materials either i) contain amphibole, which is unstable at 3 GPa, and/or ii) contain up to 4 times as much K_2O as MORB, resulting in enhanced K-white mica stability, and therefore higher melt productivity. Unaltered MORB that has undergone prograde dehydration is likely to produce <10 vol% melt. B, C) SiO_2 and K_2O contents reported for experimental melts and calculated for experimental residues; values normalized to oxide totals of 100%. Melts are always more siliceous and potassic than the starting material, so increasing melt fraction generally drives the SiO_2 and K_2O content of the residue down; the exception is the wacke, for which the SiO_2 content of the melt is essentially the same as the starting material. D) P-wave speed for residues of partial melting and melt extraction, calculated from reported mineral compositions and modes. At 3 GPa, pelite residues are 7–8 km/s, wacke 6.0–6.5 km/s, tonalite 7.0–7.5 km/s, and K-MORB or amphibolite residues are 7.5–8 km/s. E) Density of residue, calculated from reported mineral compositions and modes. Densities generally increase with degree of melt extraction. At 3 GPa, pelite residues are 3300–3400 kg/m^3, wacke 3000–3200 kg/m^3, tonalite 3100–3300 kg/m^3, and K-MORB or amphibolite residues are 3400–3600 kg/m^3.

In contrast, pelite, wacke and tonalite that reach 900–975 °C (depending on rock type) and undergo melt extraction (unfilled diamonds in Fig. 6B), have densities comparable to or less than the mantle. If they rise to the Moho (squares in Fig. 6B), these residues will have densities comparable to the lower crust. At temperatures of 950–1050 °C (depending on rock type), they will have densities comparable to or greater than the mantle; if they rise to the Moho (squares in Fig. 6B), for example because they are mixed or interlayered with more buoyant rocks as observed in UHP terrains, these residues will have densities comparable to the lower crust. MORB is gravitationally unstable with respect to mantle peridotite at 800–1050 °C, just as at 800 °C.

Thus, the calculations and experiments indicate that MORB is negatively buoyant with respect to the mantle at all temperatures at 3 GPa. All other crustal rocks that reach 900–975 °C produce large volumes of felsic melt that is buoyant and may ascend, and a refractory, high-wavespeed residue that is gravitationally stable within the mantle or at the base of the lower crust.

Experiments also show that dehydration melting of pelite, wacke and tonalite at temperatures up to 1050 °C (at 3–4 GPa) leads to Fe +

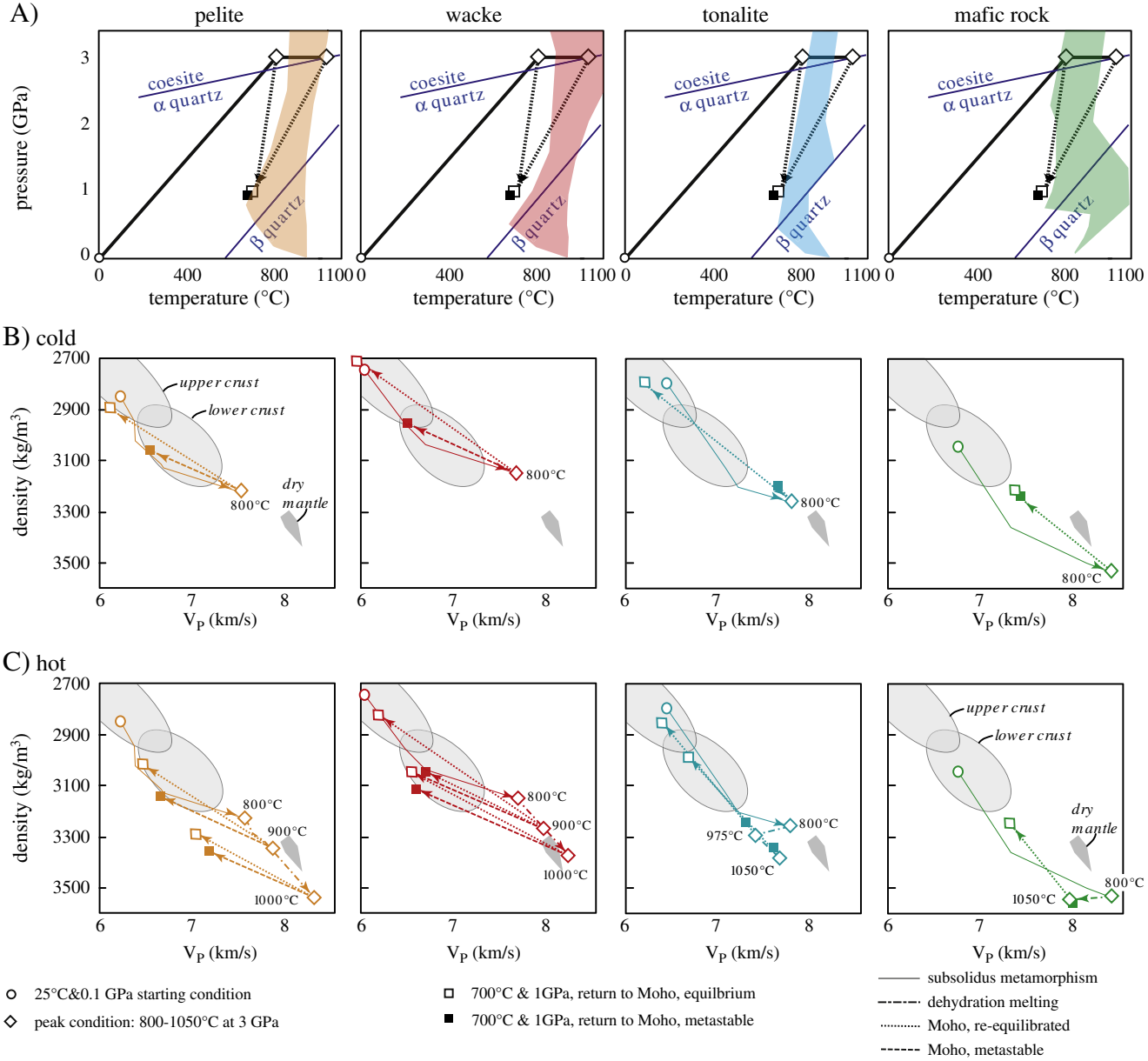

Fig. 6. Physical properties of rocks along 'cold' (800 °C) and 'hot' (1050 °C) subduction paths, followed by relamination to continental Moho conditions of 1 GPa and 700 °C. Effects of subsolidus prograde metamorphism shown by solid lines, effects of melting by dash–dot lines, effects of re-equilibration at 1 GPa and 700 °C by dotted lines, and effects of metastable return to 1 GPa and 700 °C by dashed lines. A) Cold and hot PT paths relative to dehydration-melting field (colored). B) Density–V_P evolution along the cold path. During subduction and subsolidus dehydration, quartzofeldspathic rocks increase in density and seismic velocity to values greater than those typical of the lower crust but less than those of the upper mantle, whereas mafic rocks become denser than (and as fast as) the mantle. During relamination at the Moho (1 GPa, 700 °C), mafic rocks have densities and velocities similar to the lower crust, whereas quartzofeldspathic rocks have densities and velocities typical of the crust. C) Density–V_P evolution along the hot path. During 'hot' subduction, the residues of partially melted quartzofeldspathic rocks remain less dense than the mantle up to ~900–975 °C, depending on rock type. If relaminated at the Moho all of these rocks have densities and velocities typical of the crust; if high-pressure minerals survive metastably, the densities and velocities are typical of the lower crust. At higher temperatures, the residues of partially melted quartzofeldspathic rocks can become denser and faster than the mantle if sufficient melt forms and are extracted. Gray boxes: reference values for upper and lower crust in orogens from Christensen and Mooney (Christensen and Mooney, 1995); dark gray line: calculated properties of MORB-depleted mantle (Workman and Hart, 2005) pyrolite (Ringwood, 1991), and Talkeetna arc peridotite (Table 2), from 1 GPa and 700 °C to 3 GPa and 1050 °C. Open circles show physical properties at 25 °C and 0.1 GPa. Diamonds show physical properties at maximum P and T. Squares show physical properties at 700 °C and 1 GPa. Subsolidus phase relations modeled with Perple_X, hypersolidus phase relations from experiments, and physical properties modeled with the algorithm of Hacker and Abers (Hacker and Abers, 2004). Experimental data are not available for all rocks at 3 GPa and 1050 °C, so alternative data were used: 4 GPa for the pelite and wacke, 2.1–3.2 GPa for the tonalite, and 2.2 GPa and 1050 °C for the mafic rock.

Mg enrichment and Na, K, and H_2O depletion of the residue (Fig. 5). Studies of rocks partially melted in orogenic belts at relatively low pressures (0.6–1 GPa) and temperatures (800–1000 °C) corroborate these observations and also note depletion of Ba, Rb, Cs, and U in metasedimentary residues (Bea and Montero, 1999; Fornelli et al., 2002; Guernina and Sawyer, 2003; Harris and Inger, 1992; Reid et al., 1989; Schmid, 1979; Schnetger, 1994; Solar and Brown, 2001; Watt and Harley, 1993). While it is difficult to quantify these effects, the implication is that the refractory residues of partially melted metasedimentary rocks will have K_2O contents around 1 wt.% and thus heat-production rates comparable to that shown in Fig. 3. Moreover, mixtures of residues produced by experimental melting have compositions similar to average post-Archean medium- to high-pressure granulites (Fig. 7).

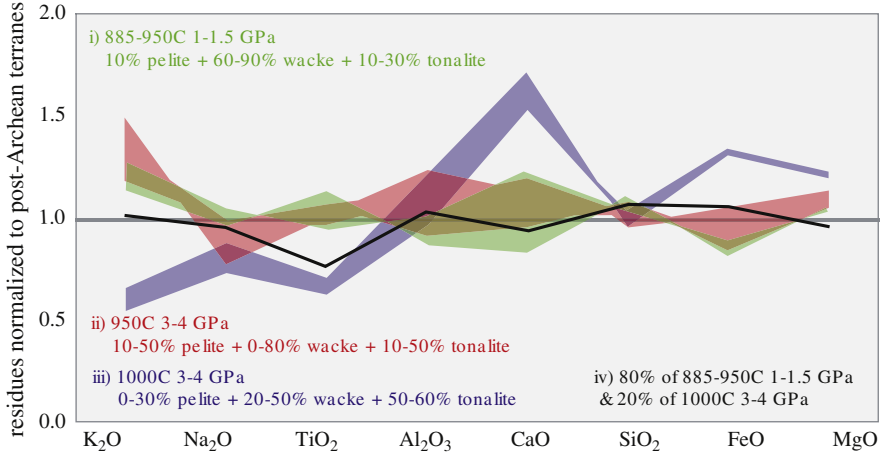

Fig. 7. Some mixtures of residues of experimentally melted crustal rocks are similar to post-Archean deep crustal sections. Mixtures of residues produced at i) 885–950 °C and 1–1.5 GPa, ii) 950 °C and 3–4 GPa, and iii) 1000 °C and 3–4 GPa are shown in separate colors. Heavy black line shows an 80/20 mix of the 'i' and 'iii' residues. Compositions are normalized—using a linear scale—to average post-Archean medium- to high-pressure granulites (updated database of Rudnick and Presper, 1990). Element order reflects decreasing compatibility in continental crust (after Hofmann, 1988). Ti is the least important element in this comparison because many experiments do not quantify abundances of Ti-bearing phases.

4. Continental relamination

If the lower continental crust is more felsic than commonly believed, and if significant proportions of the crustal rocks that are subducted remain buoyant enough to resist being recycled back into the mantle, a large amount of subducted crust could be relaminated to the base of the crust in the upper plate. Perhaps some of this material undergoes sufficient melt loss that it remains in the lower crust as a dense, high-wavespeed, and refractory—yet relatively silica rich—residue. Here we explore this possibility for four different tectonic settings.

4.1. Refining during sediment subduction

Trenches subduct significant volumes of sediment to depths greater than 50 km (Fig. 2) (Clift and Vannucchi, 2004; Reinecke, 1991; Scholl and von Huene, 2007). About 25% of this sediment is chert or carbonate (Plank and Langmuir, 1998) that will undergo minimal changes in mineralogy and volatile content during subduction (Connolly, 2005; Hacker, 2008; Kerrick and Connolly, 2001; Massonne et al., 2007). The rest, however, ranges from pelite to wacke to volcaniclastic sediment (Plank and Langmuir, 1998), and will undergo phase changes and physical property changes as described and illustrated above.

At subduction-zone conditions of 800 °C and 3 GPa, ~10% of subducting sediment is negatively buoyant with respect to the upper mantle (Behn et al., in review). The remaining 90% are positively buoyant with respect to the upper mantle and may detach from the downgoing plate and rise as diapirs through the mantle wedge to relaminate the upper plate (Behn et al., in review), either at the base of cold, high viscosity mantle "lithosphere" (Gerya and Meilick, 2011) or at the base of arc crust (Fig. 16 in 9, Behn et al., in review). We

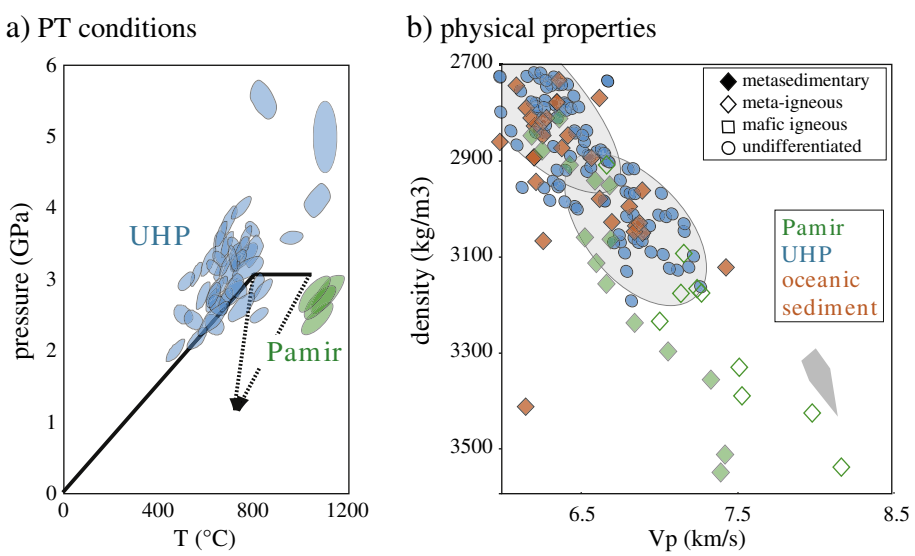

Fig. 8. a) Peak PT conditions for subduction-erosion xenoliths from the Pamir and ultrahigh-pressure terrains worldwide (PT path from Fig. 3A included for reference). b) Density and V_P for the Pamir xenoliths, UHP rocks (>55 wt.% SiO_2 only), and oceanic sediments (Plank and Langmuir, 1988) at 700 °C and 1 GPa. Values for xenoliths calculated from observed mineral abundances, measured mineral compositions, and mineral elastic data, using Hacker and Abers, (2004); values for UHP rocks calculated by applying the same algorithm to mineral modes and compositions calculated using Perple_X. Gray field for upper and lower crust and bar for mantle same as Fig. 6.

expect that the general case should be ascent of buoyant material to the base of arc crust, since high upper mantle temperatures extend to the base of the crust in arcs (Kelemen et al., 2003b) rendering viscosities low enough to permit viscous flow due to lithologic buoyancy contrasts (Jull and Kelemen, 2001). UHP xenoliths in South African and Siberian kimberlites, containing coesite-kyanite-sanidine-omphacite-garnet with metasedimentary $d^{18}O$ values, record ~1200 °C and 4 GPa (Sharp et al., 1992) consistent with conditions for diapirs passing through the mantle wedge, and with phase equilibrium experiments at these conditions (Spandler et al., 2010). Other numerical and analog models of subduction suggest that a significant fraction of subducted sediment is either (a) thrust directly into or beneath arc lower crust, or (b) underplated to the base of the arc crust following extrusion back up a "subduction channel" (Chemenda et al., 1995; Currie et al., 2007; Gerya et al., 2007; Gorczyk et al., 2006; Warren et al., 2008).

Sediments introduced into the mantle by subduction are likely to undergo divergent paths depending on whether they are felsic or mafic. Volumetrically minor, mafic sediments can become negatively buoyant with respect to upper mantle peridotite and continue to descend, whereas more-abundant, more-felsic and carbonate-rich sediments remain positively buoyant and may relaminate the base of the upper plate crust (Fig. 2A). The Swakane gneiss (Matzel et al., 2004) and the Skagit gneiss (Gordon et al., 2010; Misch, 1968) in the Washington Cascades may represent such relaminated sediments. This may help to explain why these rocks, which record peak pressures ~1 GPa (Valley et al., 2003) and are exposed today, overlie 35–40 km thick continental crust (Das and Nolet, 1998). Either these rocks were in the mid-crust in an "Andean" margin with anomalous, 60–70 km thick crust during peak metamorphism, or the lower crustal material underlying these rocks at present was emplaced there via relamination after peak metamorphism of the exposed gneisses.

4.2. Refining during arc subduction

Trenches subduct seamounts, arcs, and igneous plateaus at significant rates (Yamamoto et al., 2009). Igneous rocks in intra-oceanic arcs are composed of mafic to felsic volcanic rocks, an intermediate-composition middle crust, mafic lower crust, and a thin pyroxenite layer (e.g., Dhuime et al., 2009; Greene et al., 2006; Jagoutz et al., 2009; Kelemen et al., 2003a; Rioux et al., 2010). At the pressures and temperatures typical of active arcs, the volcanic and plutonic rocks are positively buoyant with respect to the upper mantle (Behn and Kelemen, 2006). During subduction, however, the density increase in the mafic portions of the arc crust will be sufficient to cause it to become negatively buoyant with respect to the mantle, whereas the intermediate to felsic portions of an arc (e.g., the 'wacke' component, equivalent to andesitic igneous rocks) will remain positively buoyant (Fig. 2B). Behn et al. (Behn et al., in review) showed that typical subduction-zone conditions are sufficient to cause 10^2–10^3 m-scale layers that are 200 kg/m^3 less dense than the mantle to undergo diapiric separation at temperatures <800 °C.

Thus, subducting volcanoplutonic arcs may undergo density-driven separation: the mafic igneous rocks become gravitationally unstable eclogite that is returned to the mantle, whereas the more-felsic igneous rocks remain buoyant with respect to the upper mantle and may be relaminated to the base of the crust in the overlying plate (Fig. 2B). The felsic rocks may become hot enough to produce a melt that rises to even shallower crustal levels.

4.3. Refining during subduction erosion

In about 75% of the volcanoplutonic arcs on Earth, forearc crust is being ablated by the downgoing plate (Clift and Vannucchi, 2004; Scholl and von Huene, 2007); this material must either be subducted into the deep mantle or thrust beneath the upper plate crust [Fig. 16 in 9] as is proposed for the Salinian block in central California (Barth et al., 2003). Scholl and Von Huene concluded that ~95% of this ablated rock is subducted deep into the mantle by assuming that the ablated lower crust is mafic and that global exposures of high-pressure crustal rocks are small. However, i) much forearc crust is composed of metasediments and other rocks derived from the top of the subducting plate, and from intermediate to felsic arc volcanic, volcaniclastic and plutonic rock, rather than mafic lower arc crust, ii) large volumes of (ultra)high-pressure terrains are known (see below), iii) even larger volumes of granulite facies metamorphic rocks may have gone to eclogite-facies conditions and then re-equilibrated at the base of the crust, iv) thrust imbrication of fore-arc material into arc lower crust does not require eclogite-facies conditions, and v) the mass of radiogenic ^{40}Ar in the atmosphere suggests that <30% of the continental crust has been recycled into the mantle (Coltice et al., 2000). Numerical models (Gerya and Meilick, 2011; Gerya and Stöckhert, 2006; Gerya et al., 2007; Keppie et al., 2009) also suggest that ablated crustal material may not be subducted into the asthenosphere, but may instead be relaminated to the base of the crust in the upper plate either by extrusion up the subduction channel or via diapirs through the mantle wedge.

Insight into the physical and chemical processes during subduction erosion comes from an unusual suite of 11 Ma xenoliths from the Pamir. These xenoliths encompass a broad range of lithologies, dominated by metasedimentary rocks (see Supplementary Text in Behn et al., in review for a discussion of criteria for identifying metasediments, and the outcome of such methods) and felsic to mafic meta-igneous rocks. All have eclogite-facies mineralogies, such as garnet + clinopyroxene + kyanite + K-feldspar + quartz in metapelites (Hacker et al., 2005). Zircon and monazite ages show that these rocks were derived from the Asian upper plate (Ducea et al., 2003)—i.e., they are truly products of subduction erosion. Mineral compositions reveal that the xenoliths recrystallized at ~2.7 GPa (~90 km depth) and 1050 °C (Fig. 8A), within the mantle beneath the 75 km-thick Asian crust. As these rocks were typical upper crustal rocks at the time they were tectonically eroded from the upper plate, they must have undergone massive devolatilization and melting—and concomitant changes in physical properties—during subduction (Fig. 5). Indeed, the xenoliths have calculated densities and P-wave velocities as high as ~3500 kg/m^3 and ~8.3 km/s (Fig. 8B), as expected for crustal residues of melting, and typical of the lower crust and upper mantle.

Thus, subduction erosion is capable of inducing profound changes in rock physical properties, such that mafic rocks become gravitationally unstable eclogite, and felsic rocks become positively to neutrally buoyant and rise into the lower crust or to the base of the crust in the overthrust plate (Fig. 2C). The felsic rocks are also likely to produce a melt that rises to higher crustal levels (e.g. producing the Cenozoic magmatism of the Pamir, Schwab et al., 2004).

4.4. Refining during subduction of continental crust

Metamorphic terrains containing coesite document the exhumation of continental rocks from depths of >100 km throughout the Phanerozoic, and have been interpreted to have formed during subduction of continental margins (Coleman and Wang, 1995). These so-called ultrahigh-pressure (UHP) terrains vary greatly in size, from the >30,000 km^2 terrains in Norway and China, to small kilometer-scale bodies (Ernst et al., 2007; Kylander-Clark et al., in review). All are dominated by quartzofeldspathic gneiss with a few percent mafic rock (eclogite). Some include sedimentary or rift-volcanic sequences suggesting that they were sediment-covered passive margins prior to subduction (e.g., Oberhänsli et al., 2002; Svenningsen, 2001). UHP terrains have now been discovered in most well-studied Phanerozoic continental orogenic belts (Liou et al., 2004)—

indeed, many continental orogens have undergone multiple UHP episodes (Brueckner and van Roermund, 2004).

While some felsic gneisses do record eclogite facies conditions (e.g., Oberhaensli et al., 1985) most felsic UHP rocks, have undergone such extensive retrograde metamorphism during decompression and later cooling that they preserve little or no record of metamorphism at peak pressure. Commonly, only a few mafic eclogite enclaves within felsic gneisses, and high-pressure phases locally preserved in garnets in felsic gneisses, reveal that the entire terrain was subducted to mantle depths. It is not known how many granulite terrains and even batholithic rocks were subducted to these depths and subsequently were completely overprinted without a trace of their UHP history.

Most UHP rocks were metamorphosed at peak conditions of 800 °C and 3 GPa (Fig. 8A) (Hacker, 2006). Such conditions produce significant increases in density (Massonne et al., 2007) and velocity (Fig. 8B). However, because it is dominantly felsic material, large proportions of subducting continental crust will remain buoyant with respect to the upper mantle at UHP conditions and could rise as either coherent blocks (e.g., Hacker et al., 2010), subduction channel plumes (Li and Gerya, 2009) or diapirs (Little et al., in review; Yin et al., 2007). Indeed, all UHP terrains show a post-UHP granulite- to amphibolite-facies 'Barrovian' overprint at lower crustal pressures (Banno et al., 2000; Johnston et al., 2007; Massonne and O'Brien, 2003; O'Brien and Carswell, 1993; Root et al., 2005; Simon and Chopin, 2001; Zhang et al., 1997) indicating that they ascended to lower crustal depths following subduction-zone metamorphism and remained there for a several millions of years (Kylander-Clark et al., 2008; Walsh and Hacker, 2004).

At least two UHP localities record higher temperatures: garnet-rich gneisses in the Bohemian and Kokchetav Massifs reached 1000–1200 °C at pressures of at least 4 GPa (Manning and Bohlen, 1991; Masago, 2000; Massonne, 2003). Whether such conditions are unusual or normal for subduction of continental crust is unknown, largely because of the likelihood that such rocks will not survive exhumation without complete retrogression. Such temperatures will cause extensive partial melting in felsic crustal rocks (Massonne, 2009), leading to large increases in the density and V_P of the residue if the melt is extracted (Fig. 5) (Massonne et al., 2007). At such high temperatures, dense residues of melted felsic rocks, together with mafic eclogites, may be able to separate from the more-felsic buoyant material (Fig. 2D).

5. Rates of relamination and continental refining

In each of the four tectonic settings enumerated in the previous section, subducting felsic material may be relaminated to the base of the crust in the upper plate, adding to the lower crust, while subducting mafic material may be lost into the underlying mantle through eclogitization. In the following section we present order-of magnitude estimates of continental refining rates for comparison with other processes and to determine whether these rates are sufficient to significantly affect continental evolution (Fig. 9).

The global sediment subduction flux is 1.1–1.6 km^3/yr, after a compaction correction to remove porosity (Clift and Vannucchi, 2004; Scholl and von Huene, 2007). Subducting sediment varies from 23 to 79 wt.% SiO_2, but averages 59 wt.% SiO_2 (Plank and Langmuir, 1998). Assuming a sediment density of 2500 kg/m^3 results in a global sediment-subduction SiO_2 flux of 1.7–2.4 Tg/yr. As noted above, 90% of these rocks will be positively buoyant with respect to the upper mantle and may rise to relaminate the base of the crust in the upper

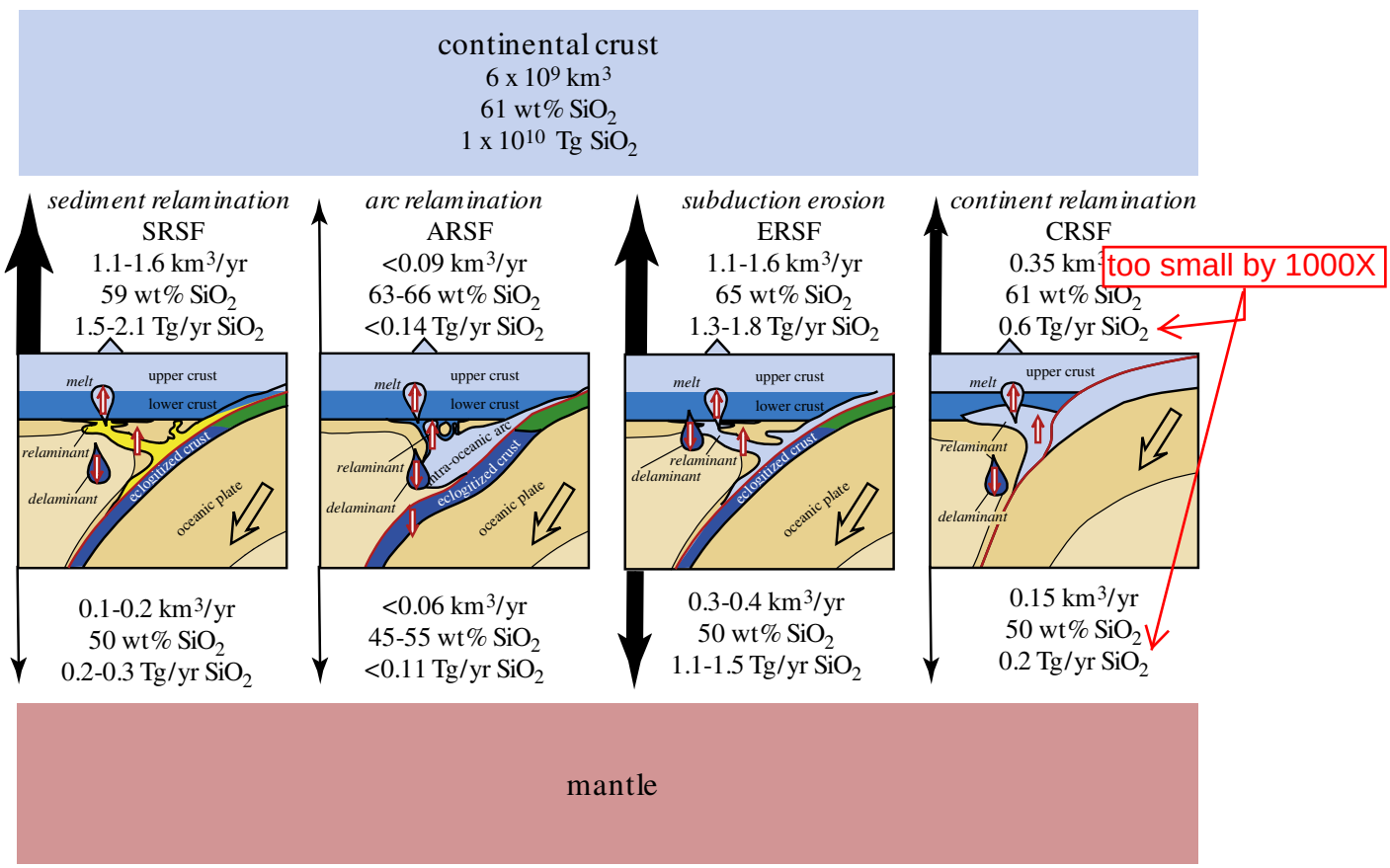

Fig. 9. Calculated material fluxes suggest that continental relamination may be i) dominated by subduction erosion > sediment subduction ≫ continent subduction > arc subduction, and ii) capable of refining the composition of the continental crust on a 2 Ga timescale.

plate, producing a possible sediment-relamination SiO_2 flux (SRSF) of 1.5–2.1 Tg/yr. About 10% of subducting sediments, with a SiO_2 content around 50 wt.%, may be returned to the mantle, resulting in a SiO_2 flux back into the mantle of 0.2–0.3 Tg/yr.

It is difficult to estimate the global average arc subduction rate (wherein the arc is part of the subducting plate, distinct from subduction erosion of the upper plate). The current length of intra-oceanic arcs is ~10,000 km. The mean intra-oceanic arc age (average age of arc initiation, weighted by arc length) is ~65 Myr and the weighted mean arc cross section is 2000 km^2 (data from Reymer and Schubert, 1984). If total arc length and arc subduction/accretion rates have been constant during the past 65 Myr, intra-oceanic arcs have been created at a rate of 0.15 km^3/yr. This sets an upper limit to the arc subduction rate, as an unknown fraction of this material has been accreted to plate margins. About half of intra-oceanic arc crust is felsic, with an average SiO_2 content of 63–66 wt.% (calculated for the Talkeetna arc, Hacker et al., 2008). Assuming a rock density of 2800 kg/m^3 results in an upper bound on the SiO_2 flux of 0.14 Tg/yr for the felsic portions of subducted intra-oceanic arcs (arc-relamination SiO_2 flux, ARSF). All of this felsic material could be relaminated. The other, mafic half of intra-oceanic arcs, with ~45–55 wt.% SiO_2 and a density of ~3000 kg/m^3 may be returned to the mantle upon eclogitization, resulting in an upper bound on the SiO_2 flux back into the mantle of 0.11 Tg/yr.

The global average subduction erosion rate is ~1.4–2.0 km^3/yr (Clift and Vannucchi, 2004; Scholl and von Huene, 2007). About 25% of this occurs in intra-oceanic arcs and ~75% in continental arcs; above we assumed that intra-oceanic arcs are 50% mafic, here we assume that continental arcs are the same. Assuming that the felsic portions of arcs contain ~63–66 wt.% SiO_2, have a density of 2800 kg/m^3, and are all relaminated, results in a possible subduction-erosion relamination SiO_2 flux (ERSF) of ~1.3–1.8 Tg/yr for felsic rocks. The mafic portions of eroding arcs, with ~50 wt.% SiO_2 and a density of 3000 kg/m^3, may be returned to the mantle as eclogite, resulting in a SiO_2 flux back into the mantle of 1.1–1.5 Tg/yr.

To estimate the rate of continent-collision subduction, consider the modern Alpine–Himalayan orogen, which constitutes the major Cenozoic collisional zone. This orogen is ~10,000 km long. Tertiary shortening is ~500 km in the Alps (Schmid et al., 1996), and ~2750 km in the Himalaya (Dewey et al., 1989). If a 25-km thick crustal section was subducted a mere 100 km beyond Moho depth along the length of the Alpine–Himalayan chain over the last 50 Myr, this yields a volume of $\sim 2.5\times10^7$ km^3 or a an average rate of ~0.5 km^3/yr. Assuming that continental crust contains ~61 wt.% SiO_2 (Rudnick and Gao, 2003) or more (this paper) and has a density of 2800 kg/m^3, results in a possible continent-relamination SiO_2 flux (CRSF) of ~0.6 Tg/yr. Some unknown fraction of mafic material (shown as 25% in Fig. 9) is returned to the mantle.

The present volume of continental crust on Earth is $\sim 6\times10^9$ km^3, corresponding to an SiO_2 mass of 1×10^{10} Tg for a density of 2800 kg/m^3 and a SiO_2 concentration of 60–65 wt.%. The estimates from the previous four paragraphs imply that felsic crustal material—with sufficiently low density to remain buoyant with respect to the upper mantle—carries SiO_2 into subduction zones at a rate >3.5 Tg/yr (>1.5 SRSF + >0.1 ARSF + >1.3 ERSF + >0.6 CRSF). If all of this buoyant subducted material is relaminated to the underside of the continental crust, the entire crust could have been relaminated in ~2.7 Ga. During the same period, a SiO_2 flux of ~1.8 Tg/yr may have been returned to the mantle. This has negligible effect on the composition of the upper mantle, which has $\sim 5\times10^{11}$ Tg SiO_2 (mantle densities and composition from Kennett et al., 1995; McDonough and Sun, 1995).

While our paper demonstrates that present-day subduction and recycling fluxes are more than sufficient to process the existing volume of continental crust, our analysis does not allow us to determine when relamination processes became important in continental evolution. Obviously, if subduction did not occur in the Hadean or Archean, the relamination processes we describe would not have been active. Also, it is evident that recycling of continental sediments could not have occurred before the initial generation of continental crust.

6. Limitations of the relamination model

There are several limitations to our relamination model for crustal differentiation in subduction zones. Here we list a few.

1. Fluid-fluxed melting is ignored. However, porosities are so low in metamorphic rocks and H_2O solubilities in silicate melts are so high that the amount of melt produced by fluid-fluxed melting may be minor.
2. Decompression melting is ignored. This will generate only small amounts of melt in rocks already depleted by high pressure melting at temperatures as high as 1100 °C, but will produce large amounts of melt in fertile lithologies, for example when cold, felsic diapirs heat and decompress as they ascend through the mantle wedge (Fig. 5).
3. Relatively few dehydration-melting experiments have been conducted and melt activity models are still insufficiently accurate.
4. The effects of secular variation in Earth tectonics are ignored. If, for example, continental subduction did not occur during the Precambrian, our rate calculations cannot be extended to Archean times.
5. The direct effects of weathering on crustal differentiation (Albarede and Michard, 1986; Lee et al., 2008; Taylor and McLennan, 1985)—have been ignored, although weathering is implicit in our model as it is the means by which sediment is produced, and the process that produces peraluminous pelitic sediments from metaluminous protoliths.

7. Tests of the relamination model

Potential tests of the relamination model could derive from secular variation in certain isotopic systems, such as Pb, or from field studies. For example, do large metasedimentary terrains or xenoliths suites show an inverse relationship between detrital zircon age and paleo-depth? Locations in which to assess this include the Washington Cascades (as noted above), the Pelona–Orocopia–Rand-type schists of California and Arizona (e.g., Barth et al., 2003), or the Catalina Schist of southern California (Kimbrough and Grove, 2007). What fraction of Barrovian metamorphic sequences have an earlier UHP history, indicating relamination of subducted continental material? What fraction of UHP terranes were not subducted and exhumed as coherent sheets (Andersen et al., 1991), but instead rose as diapirs (Little et al., in press; Yin et al., 2007)?

8. Conclusions

The composition of the lower continental crust is incompletely constrained; it has been inferred—on the basis of heat flow and xenolith compositions—to be relatively mafic, but a review of the available constraints indicates that the middle and lower crust together could contain significant volumes of felsic rocks and have an average SiO_2 content as high as 64 wt.%. In subduction zones sensu lato, rocks undergo prograde metamorphism, partial melting, and melt extraction processes that lead to moderate increases in seismic velocity and density for most rocks, and to major increases in velocity and density for mafic rocks. The end result is that mafic rocks are dense enough to sink within the mantle, whereas felsic rocks are positively to neutrally buoyant and can relaminate the base of the upper plate crust. This can take place during sediment subduction, subduction erosion, subduction of arc crust, and subduction of continental crust. Estimated mass fluxes for these processes are sufficiently large that they could have refined the composition of the entire continental crust over the lifetime of Earth, leading to the present composition of the crust.

Acknowledgments

Roberta Rudnick graciously provided an updated database of post-Archean granulite terrain compositions and lower-crustal xenolith compositions, supplementing the landmark study of Rudnick and Presper (1990). Mike Brown generously pointed us to the right literature on melting of natural rocks. Reviews by Taras Gerya, Nina Simon, and anonymous reviewer were helpful in improving the presentation of the manuscript. This material is based upon work supported by National Science Foundation grant OCE-0646734.

References

Albarede, F., Michard, A., 1986. Transfer of continental Mg, S, O and U to the mantle through hydrothermal alteration of the oceanic-crust. Chem. Geol. 57, 1–15.

Andersen, T.B., Jamtveit, B., Dewey, J.F., Swensson, E., 1991. Subduction and eduction of continental crust: major mechanism during continent-continent collision and orogenic extensional collapse, a model based on the south Caledonides. Terra Nova 3, 303–310.

Armstrong, R.L., 1981. Radiogenic isotopes — the case for crustal recycling on a near-steady-state no-continental-growth earth. Philos. Transact. R. Soc. A Math. Phys. Eng. Sci. 301, 443–472.

Arndt, N.T., Goldstein, S.L., 1989. An open boundary between lower continental crust and mantle; its role in crust formation and crustal recycling. Tectonophysics 161 (3–4), 201–212.

Auzanneau, E., Vielzeuf, D., Schmidt, M.W., 2006. Experimental evidence of decompression melting during exhumation of subducted continental crust. Contrib. Mineral. Petrol. 152 (2), 125–148.

Banno, S., Enami, M., Hirajima, T., Ishiwatari, A., Wang, Q., 2000. Decompression P–T path of coesite eclogite to granulite from Weihai, eastern China. Lithos 52, 97–108.

Barth, A.P., Wooden, J.L., Grove, M., 2003. U–Pb zircon geochronology of rocks in the Salinas Valley region of California: a reevaluation of the crustal structure and origin of the Salinian block. Geology 31, 517–520.

Bea, F., Montero, P., 1999. Behavior of accessory phases and redistribution of U, Th, Zr, REE and Y during metamorphism and partial melting of metapelites in the lower crust: an example from the Kinzigite Formation of Ivrea-Verbano, NW Italy. Geochim. Cosmochim. Acta 63, 1133–1153.

Behn, M.D., Kelemen, P.B., 2003. Relationship between seismic P-wave velocity and the composition of anhydrous igneous and meta-igneous rocks. G-cubed 4, article 1041.

Behn, M.D., Kelemen, P.B., 2006. The stability of arc lower crust: insights from the Talkeetna arc section, south-central Alaska and the seismic structure of modern arcs. J. Geophys. Res. 111, B11207. doi:10.1029/2006JB004327.

M.D. Behn, P.B. Kelemen, G. Hirth, B.R. Hacker and H.J. Massonne, in review, Sediment diapirs and arc magmatism, Nature Geoscience.

Brown, M., 2007. Crustal melting and melt extraction, ascent and emplacement in orogens; mechanisms and consequences. J. Geol. Soc. Lond. 164 (4), 709–730.

Brueckner, H.K., van Roermund, H.L.M., 2004. Dunk tectonics: a multiple subduction/eduction model for the evolution of the Scandinavian Caledonides. Tectonics 23, 1–20.

Chemenda, A.I., Mattauer, M., Malavieille, J., Bokun, A.N., 1995. A mechanism for syn-collisional rock exhumation and associated normal faulting: results from physical modelling. Earth & Planet. Sci. Lett. 132, 225–232.

Christensen, N.I., Mooney, W.D., 1995. Seismic velocity structure and composition of the continental crust: a global view. J. Geophys. Res. 100, 9761–9788.

Clift, P., Vannucchi, P., 2004. Controls on tectonic accretion versus erosion in subduction zones: implications for the origin and recycling of the continental crust. Rev. Geophys. 42. doi:10.1029/2003RG000127.

Coleman, R.G., Wang, X., 1995. Ultrahigh Pressure Metamorphism. 528 pp. Cambridge University Press, New York.

Coltice, N., Albarede, F., Gillet, P., 2000. (super 40) K- (super 40) Ar constraints on recycling continental crust into the mantle. Science 288 (5467), 845–847.

Connolly, J.A.D., 1990. Multivariable phase diagrams an algorithm based on generalized thermodynamics. Am. J. Sci. 290, 666–718.

Connolly, J.A.D., 2005. Computation of phase equilibria by linear programming: a tool for geodynamic modeling and its application to subduction zone decarbonation. Earth & Planet. Sci. Lett. 236, 524–541.

Currie, C.A., Beaumont, C., Huismans, R.S., 2007. The fate of subducted sediments: a case for backarc intrusion and underplating. Geology 35, 1111–1114.

Das, T., Nolet, G., 1998. Crustal thickness map of the western United States by partitioned waveform inversion. J. Geophys. Res. 103, 30021–30038.

DeBari, S.M., Sleep, N.H., 1991. High-Mg, low-Al bulk composition of the Talkeetna island arc, Alaska: implications for primary magmas and the nature of arc crust. Geol. Soc. Am. Bull. 103, 37–47.

Dewey, J.F., Cande, S., Pitman, W.C., 1989. Tectonic evolution of the India/Eurasia collision zone. Eclogae Geologica Helvetica 82, 717.

Dhuime, B., Bosch, D., Garrido, C.J., Bodinier, J.-L., Bruguier, O., Hussain, S.S., Dawood, H., 2009. Geochemical Architecture of the Lower- to Middle-crustal Section of a Paleo-island Arc (Kohistan Complex, Jijal-Kamila Area, Northern Pakistan): implications for the Evolution of an Oceanic Subduction Zone. J. Petrol. 50, 531–569.

Ducea, M.N., Lutkov, V., Minaev, V.T., Hacker, B., Ratschbacher, L., Luffi, P., Schwab, M., Gehrels, G.E., McWilliams, M., Vervoort, J., Metcalf, J., 2003. Building the Pamirs: the view from the underside. Geology 31, 849–852.

Ernst, W.G., Boettcher, A.L., Newton, R.C., 1980. Mineral paragenesis in Franciscan metagraywackes of the Nacimiento Block, a subduction complex of the Southern California Coast Ranges. J. Geophys. Res. 85 (B12), 7045–7055.

Ernst, W.G., Hacker, B.R., Liou, J.G., 2007. Petrotectonics of ultrahigh-pressure crustal and upper-mantle rocks: implications for Phanerozoic collisional orogens. Geol. Soc. Am. Spec. Pap. 433, 27–49.

Ferry, J.M., 1982. A comparative geochemical study of pelitic schists and metamorphosed carbonate rocks from south-central Maine, USA. Contrib. Mineral. Petrol. 80, 59–72.

Fornelli, A., Piccarreta, G., Del Moro, A., Acquafredda, P., 2002. Multi-stage melting in the lower crust of the Serre (southern Italy). J. Petrol. 43 (12), 2191–2217.

Fuhrman, M.L., Lindsley, D.H., 1988. Ternary-feldspar modeling and thermometry. Am. Mineral. 73, 201–215.

Gerya, T.V., Meilick, F.I., 2011. Geodynamic regimes of subduction under an active margin: effects of rheological weakening by fluids and melts. J. Metamorph. Geol. 29, 7–31.

Gerya, T.V., Stöckhert, B., 2006. Two-dimensional numerical modeling of tectonic and metamorphic histories at active continental margins. Int. J. Earth Sci. 95, 250–274.

Gerya, T.V., Yuen, D.A., 2003. Rayleigh-Taylor instabilities from hydration and melting propel 'cold plumes' at subduction zones. Earth & Planet. Sci. Lett. 212, 47–62.

Gerya, T.V., Perchuk, L.L., Burg, J.-P., 2007. Transient hot channels: perpetrating and regurgitating ultrahigh-pressure, high temperature crust-mantle associations in collision belts. Lithos 103, 236–256.

Gorczyk, W., Gerya, T.V., Connolly, J.A.D., Yuen, D.A., Rudolph, M., 2006. Large-scale rigid-body rotation in the mantle wedge and its implications for seismic tomography. G-cubed 7. doi:10.1029/2005GC001075.

Gordon, S.M., Bowring, S.A., Whitney, D.L., Miller, R.B., McLean, N., 2010. Time scales of metamorphism, deformation, and crustal melting in a continental arc, North Cascades USA. Geol. Soc. Am. Bull. 122, 1308–1330. doi:10.1130/B30060.1.

Greene, A.R., DeBari, S.M., Kelemen, P.B., Blusztajn, J., Clift, P.D., 2006. A detailed geochemical study of island arc crust: the Talkeetna Arc section, South-central Alaska. J. Petrol. 47, 1051–1093.

Guernina, S., Sawyer, E.W., 2003. Large-scale melt-depletion in granulite terranes; an example from the Archean Ashuanipi Subprovince of Quebec. J. Metamorph. Geol. 21 (2), 181–201.

Hacker, B.R., 2006. Pressures and temperatures of ultrahigh-pressure metamorphism: implications for UHP tectonics and H2O in subducting slabs. Int. Geol. Rev. 48, 1053–1066.

Hacker, B.R., 2008. H2O subduction beyond arcs. Geochem. Geophys. Geosyst. 9. doi:10.1029/2007GC00170.

Hacker, B.R., Abers, G.A., 2004. Subduction Factory 3. An Excel worksheet and macro for calculating the densities, seismic wave speeds, and H2O contents of minerals and rocks at pressure and temperature. Geochem. Geophys. & Geosyst. 5, Q01005. doi:10.1029/2003GC000614.

Hacker, B.R., Luffi, P., Lutkov, V., Minaev, V., Ratschbacher, L., Plank, T., Ducea, M., Patiño-Douce, A., McWilliams, M., Metcalf, J., 2005. Near-ultrahigh pressure processing of continental crust: Miocene crustal xenoliths from the Pamir. J. Petrol. 46, 1661–1687.

Hacker, B.R., Mehl, L., Kelemen, P.B., Rioux, M., Behn, M.D., Luffi, P., 2008. Reconstruction of the Talkeetna intra-oceanic arc of Alaska through thermobarometry. J. Geophys. Res. 113. doi:10.1029/2007JB005208.

Hacker, B.R., Andersen, T.B., Johnston, S., Kylander-Clark, A.R.C., Peterman, E., Walsh, E.O., Young, D., 2010. High-temperature deformation during continental-margin subduction & exhumation: the Ultrahigh-Pressure Western Gneiss Region of Norway. Tectonophysics 480, 149–171.

Harris, N.B.W., Inger, S., 1992. Trace element modelling of pelite-derived granites. Contrib. Mineral. Petrol. 110, 45–56.

Herzberg, C.T., Fyfe, W.S., Carr, M.J., 1983. Density constraints on the formation of the continental Moho and crust. Contrib. Mineral. Petrol. 84 (1), 1–5.

Hilde, T.W.C., 1983. Sediment subduction versus accretion around the Pacific. Tectonophysics 99, 381–397.

Hofmann, A., 1988. Chemical differentiation of the Earth: the relationship between mantle, continental crust, and oceanic crust. Earth & Planet. Sci. Lett. 90, 297–314.

Holbrook, W.S., Mooney, W.D., Christensen, N.I., Holbrook, W.S., Mooney, W.D., Christensen, N.I., 1992. The seismic velocity structure of the deep continental crust. In: Fountain, D.M., Arculus, R., Kay, R.W., Fountain, D.M., Arculus, R., Kay, R.W. (Eds.), Continental lower crust, Developments in Geotectonics. Developments in Geotectonics, 23. Elsevier, New York, pp. 1–42.

Holland, T.J.B., Powell, R., 1996. Thermodynamics of order–disorder in minerals; II, Symmetric formalism applied to solid solutions. Am. Mineral. 81, 1425–1437.

Holland, T.J.B., Powell, R., 1998. An internally consistent thermodynamic data set for phases of petrological interest. J. Metamorph. Geol. 16, 309–343.

Holland, T., Baker, J., Powell, R., 1998. Mixing properties and activity-composition relationships of chlorites in the system MgO–FeO–Al2O3–SiO2–H2O. Earth & Planet. Sci. Lett. 10, 395–406.

Jagoutz, O.E., Burg, J.-P., Hussain, S., Dawood, H., Pettke, T., Iizuka, T., Maruyama, S., 2009. Construction of the granitoid crust of an island arc part I: Geochronological and geochemical constraints from the plutonic Kohistan (NW Pakistan). Contrib. Mineral. Petrol. 158. doi:10.1007/s00410-009-0408-3.

Jaupart, C., Mareschal, J.-C., 2003. Constraints on crustal heat production from heat flow data. In: Holland, H.D., Turekian, K.K., Rudnick, R.L. (Eds.), The Crust. Treatise on Geochemistry, 3. Elsevier-Pergamon, Oxford.

Johnston, S., Hacker, B.R., Ducea, M.N., 2007. Exhumation of ultrahigh-pressure rocks beneath the Hornelen segment of the Nordfjord-Sogn Detachment Zone, western Norway. Geol. Soc. Am. Bull. 119, 1232–1248.

Jull, M., Kelemen, P.B., 2001. On the conditions for lower crustal convective instability. J. Geophys. Res. 106, 6423–6445.

Kay, R.W., Kay, S.M., 1991. Creation and destruction of lower continental crust. Geologische Rundschau 80, 259–278.
Kelemen, P., 1995. Genesis of high Mg# andesites and the continental crust. Contrib. Mineral. Petrol. 120, 1–19.
Kelemen, P.B., Hanghøj, K., Greene, A., 2003a. One view of the geochemistry of subduction-related magmatic arcs, with an emphasis on primitive andesite and lower crust. In: Holland, H.D., Turekian, K.K., Rudnick, R.L. (Eds.), The Crust. Treatise on Geochemistry, 3. Elsevier-Pergamon, Oxford, pp. 593–659.
Kelemen, P.B., Parmentier, E.M., Rilling, J., Mehl, L., Hacker, B.R., 2003b. Thermal structure due to solid-state flow in the mantle wedge beneath arcs. Am. Geophys. Union Monogr. 138, 293–311.
Kennett, B.L.N., Engdahl, E.R., B.R., 1995. Constraints on seismic velocities in the Earth from travel times. Geophys. J. Int. 122, 108–124.
Keppie, K.D., Currie, C.A., Warren, C.J., 2009. Subduction erosion modes: comparing finite element numerical models with the geological record. Earth & Planet. Sci. Lett. 287, 241–254.
Kerrick, D.M., Connolly, J.A.D., 2001. Metamorphic devolatilization of subducted marine sediments and the transport of volatiles into the Earth's mantle. Nature 411, 293–296.
Kimbrough, D.L., Grove, M., 2007. Evidence for rapid recycling of subduction erosion forearc material into Cordilleran TTG batholiths: insight from the Peninsular Ranges of southern and Baja California, Eos. Trans. Am. Geophys. Union 88, T11B–T0581B.
Kylander-Clark, A.R.C., Hacker, B.R., Mattinson, J.M., 2008. Slow exhumation of UHP terranes: titanite and rutile ages of the Western Gneiss Region, Norway. Earth & Planet. Sci. Lett. 272, 531–540.
A. Kylander-Clark, B. Hacker and C. Mattinson, in review, Secular Evolution in Continental Subduction and Exhumation?, Geology.
Lee, C.T.A., Morton, D.M., Little, M.G., Kistler, R., Horodyskyj, U.N., Leeman, W.P., Agranier, A., 2008. Regulating continent growth and composition by chemical weathering. Proc. Natl. Acad. Sci. 105, 4981–4986.
Li, Z., Gerya, T.V., 2009. Polyphase formation and exhumation of high- to ultrahigh-pressure rocks in continental subduction zone; numerical modeling and application to the Sulu ultrahigh-pressure terrane in eastern China. J. Geophys. Res. 114 (B9).
Liou, J.G., Tsujimori, T., Zhang, R.Y., Katayama, I., Maruyama, S., 2004. Global UHP metamorphism and continental subduction/collision: the Himalayan model. Int. Geol. Rev. 46, 1–27.
T.A. Little, B.R. Hacker, S.M. Gordon, S.L. Baldwin, P.G. Fitzgerald, S. Ellis and M. Korchinski, in press, Diapiric Exhumation of Earth's youngest (UHP) eclogites in the gneiss domes of the D'Entrecasteaux Islands, Papua New Guinea, Tectonophysics.
T.A. Little, B.R. Hacker, S.M. Gordon, S.L. Baldwin, P.G. Fitzgerald, S. Ellis and M. Korchinski, in review, Diapiric Exhumation of Earth's youngest (UHP) eclogites in the gneiss domes of the D'Entrecasteaux Islands, Papua New Guinea, Tectonophysics.
Manning, C.E., Bohlen, S.R., 1991. The reaction titanite + kyanite = anorthite + rutile and titanite-rutile barometry in eclogites. Contrib. Mineral. Petrol. 109, 1–9.
Martin, H., 1986. Effect of steeper Archean geothermal gradient on geochemistry of subduction-zone magmas. Geology 14, 753–756.
Masago, H., 2000. Metamorphic petrology of the Barchi-Kol metabasites, western Kokchetav ultrahigh-pressure–high-pressure massif, northern Kazakhstan. The Island Arc 9, 358–378.
Massonne, H.-J., 2003. A comparison of the evolution of diamondiferous quartz-rich rocks from the Saxonian Erzgebirge and the Kokchetav Massif: are so-called diamondiferous gneisses magmatic rocks? Earth & Planet. Sci. Lett. 216, 347–364.
Massonne, H.J., 2009. Hydration, dehydration, and melting of metamorphosed granitic and dioritic rocks at high- and ultrahigh-pressure conditions. Earth & Planet. Sci. Lett. 288 (1–2), 244–254.
Massonne, H.J., O'Brien, P.J., 2003. The Bohemian Massif and the NW Himalaya. EMU Notes in Mineral. 5, 145–187.
Massonne, H.J., Willner, A.P., Gerya, T.V., 2007. Densities of metapelitic rocks at high to ultrahigh pressure conditions: what are the geodynamic consequences? Earth & Planet. Sci. Lett. 256, 12–27.
Matzel, J.E.P., Bowring, S.A., Miller, R.B., 2004. Protolith age of the Swakane Gneiss, north Cascades, Washington; evidence of rapid underthrusting of sediments beneath an arc. Tectonics 23 (6), 18.
McDonough, W.F., Sun, S.-s., 1995. The composition of the Earth. Chem. Geol. 120, 223–254.
Misch, P., 1968. Plagioclase compositions and non-anatectic origin of migmatitic gneisses in Northern Cascade Mountains of Washington State. Contrib. Mineral. Petrol. 17 (1), 1–70.
Montel, J.M., Vielzeuf, D., 1997. Partial melting of metagreywackes, Part II. Compositions of minerals and melts. Contrib. Mineral. Petrol. 128, 176–196.
Nesbitt, H.W., Young, G.M., 1984. Prediction of some weathering trends of plutonic and volcanic rocks based on thermodynamic and kinetic considerations. Geochim. Cosmochim. Acta 48 (7), 1523–1534.
Nockolds, S.R., 1954. Average chemical compositions of some igneous rocks. Geol. Soc. Am. Bull. 65 (10), 1007–1032.
O'Brien, P.J., Carswell, D.A., 1993. Tectonometamorphic evolution of the Bohemian Massif: evidence from high-pressure metamorphic rocks. Geologische Rundschau 82, 531–555.
Oberhaensli, R., Hunziker, J.C., Martinotti, G., Stern, W.B., 1985. Geochemistry, geochronology and petrology of Monte Mucrone; an example of Eo-Alpine eclogitization of Permian granitoids in the Sesia-Lanzo Zone, Western Alps, Italy. Chem. Geol. 52 (2), 165–184.
Oberhänsli, R., Martinotti, G., Schmid, R., Liu, X., 2002. Preservation of primary volcanic textures in the ultrahigh-pressure terrain of Dabie Shan. Geology 30, 609–702.
Pakiser, L.C., Robinson, R., 1966. Composition and evolution of the continental crust as suggested by seismic observations. Tectonophysics 3, 547–557.
Patiño Douce, A.E., 2005. Vapor-absent melting of tonalite at 15–32 kbar. J. Petrol. 46, 275–290.
Patiño Douce, A.E., Harris, N., 1998. Experimental constraints on Himalayan Anatexis. J. Petrol. 39, 689–710.
Pearce, J.A., 1976. Statistical analysis of major element patterns in basalts. J. Petrol. 17, 15–43.
Pettijohn, F.J., 1963. Chemical composition of sandstones-excluding carbonate and volcanic sands, In: Fleischer, M. (Ed.), Data of Geochemistry, sixth edition. U. S. Geological Survey Professional Paper 440-S, 21 pp.
Plank, T., Langmuir, C.H., 1988. An evaluation of the global variations in the major-element chemistry of arc basalts. Earth & Planet. Sci. Lett. 90, 349–370.
Plank, T., Langmuir, C.H., 1998. The chemical composition of subducting sediment and its consequences for the crust and mantle. Chem. Geol. 145, 325–394.
Powell, R., Holland, T., 1999. Relating formulations of the thermodynamics of mineral solid solutions; activity modeling of pyroxenes, amphiboles, and micas. Am. Mineral. 84, 1–14.
Rapp, R.P., Watson, E.B., 1991. Partial melting of amphibolite/eclogite and the origin of Archean trondhjemites and tonalites. Precambrian Res. 51, 1–25.
Rapp, R.P., Watson, E.B., 1995. Dehydration melting of metabasalt at 8–32 kbar: implications for continental growth and crust–mantle recycling. J. Petrol. 36, 893–931.
Reid, M.R., Hart, S.R., Padovani, E.R., Wandless, G.A., 1989. Contribution of metapelitic sediments to the composition, heat production, and seismic velocity of the lower crust of southern New Mexico, U.S.A. Earth & Planet. Sci. Lett. 95 (3–4), 367–381.
Reinecke, T., 1991. Very-high-pressure metamorphism and uplift of cœsite-bearing sediments from the Zermatt-Saas zone, Western Alps. Eur. J. Mineral. 3, 7–17.
Reymer, A., Schubert, G., 1984. Phanerozoic addition rates to the continental crust and crustal growth. Tectonics 3, 63–77.
Ringwood, A.E., 1991. Phase transformations and their bearing on the constitution and dynamics of the mantle. Geochim. Cosmochim. Acta 55 (8), 2083–2110.
Ringwood, A.E., Green, D.H., 1966. An experimental investigation of the gabbro-eclogite transformation and some geophysical implications. Tectonophysics 3, 383–427.
Rioux, M., Mattinson, J., Hacker, B., Kelemen, P., Blusztajn, J., Hanghøj, K., Gehrels, G., 2010. Intermediate to felsic middle crust in the accreted Talkeetna arc, the Alaska Peninsula and Kodiak Island, Alaska: an analogue for low-velocity middle crust in modern arcs. Tectonics 29, TC3001. doi:10.1029/2009TC002541.
Rollinson, H.R., Windley, B.F., 1980. An Archaean granulite-grade tonalite-trondhjemite-granite suite from Scourie, NW Scotland; geochemistry and origin. Contrib. Mineral. Petrol. 72 (3), 265–281.
Root, D.B., Hacker, B.R., Gans, P., Eide, E., Ducea, M., Mosenfelder, J., 2005. Discrete ultrahigh-pressure domains in the Western Gneiss Region, Norway: implications for formation and exhumation. J. Metamorph. Geol. 23, 45–61.
Rudnick, R.L., Fountain, D.M., 1995. Nature and composition of the continental crust: a lower crustal perspective. Rev. Geophys. 33, 267–309.
Rudnick, R.L., Gao, S., 2003. Composition of the continental crust. In: Holland, H.D., Turekian, K.K., Rudnick, R.L. (Eds.), The Crust. Treatise on Geochemistry, 3. Elsevier-Pergamon, Oxford, pp. 1–64.
Rudnick, R., Presper, T., 1990. Geochemistry of intermediate- to high-pressure granulites. In: Vielzeuf, D., Vidal, P. (Eds.), Granulites and Crustal Evolution. Kluwer Academic, Norwell, MA, pp. 523–550.
Schmid, R., 1979. Are the metapelites of the Ivrea-Verbano zone restites? Memorie di Scienze Geologiche XXXIII, 67–69.
Schmid, S.M., Pfiffner, O.A., Froitzheim, N., Schoenborn, G., Kissling, E., 1996. Geophysical–geological transect and tectonic evolution of the Swiss–Italian Alps. Tectonics 15, 1036–1064.
Schmidt, M.W., 1993. Phase relations and compositions in tonalite as a function of pressure: An experimental study at 650 °C. Am. J. Sci. 293, 1011–1060.
Schmidt, M.W., Vielzeuf, D., Auzanneau, E., 2004. Melting and dissolution of subducting crust at high pressures: the key role of white mica. Earth & Planet. Sci. Lett. 228, 65–84.
Schnetger, B., 1994. Partial melting during the evolution of the amphibolite- to granulite-facies gneisses of the Ivrea Zone, northern Italy. Chem. Geol. 113 (1–2), 71–101.
Scholl, D.W., von Huene, R., 2007. Crustal recycling at modern subduction zones applied to the past—issues of growth and preservation of continental basement, mantle geochemistry, and supercontinent reconstruction. 4D Framework of Continental Crust, edited by In: Robert, J., Hatcher, D., Carlson, M.P., McBride, J.H., Catalán, J.R.M. (Eds.), Geological Society of America, Memoir: Geological Society of America, Boulder, 200, pp. 9–32.
Schwab, M., Ratschbacher, L., Siebel, W., McWilliams, M., Lutkov, V., Minaev, V., Chen, F., Stanek, K., Nelson, B., Frisch, W., Wooden, J.L., 2004. Assembly of the Pamirs: age and origin of magmatic belts from the southern Tien Shan to the southern Pamirs and their relation to Tibet. Tectonics 23, TC4002. doi:10.1029/2003TC001583.
Semprich, J., Simon, N.S.C., Podladchikov, Y.Y., 2010. Density variations in the thickened crust as a function of pressure, temperature, and composition. Int. J. Earth Sci. 99 (7), 1487–1510.
Sen, C., Dunn, T., 1994. Dehydration melting of a basaltic compositions amphibolite at 1.5 and 2.0 GPa: implications for the origin of adakites. Contrib. Mineral. Petrol. 117, 394–409.
Sharp, Z.D., Essene, E.J., Smyth, J.R., 1992. Ultra-high temperatures and pressures from oxygen isotope thermometry of a coesite–sanidine grospydite. Contrib. Mineral. Petrol. 112, 358–370.
Shaw, D.M., 1956. Major elements and general geochemistry, Part 3 of Geochemistry of pelitic rocks. Geol. Soc. Am. Bull. 67 (7), 919–934.
Sheraton, J.W., Collerson, K.D., 1983. Archaean and Proterozoic geological relationships in the Vestfold Hills-Prydz Bay area. Antarctica. BMR J. Aust. Geol. Geophys. 8 (2), 119–128.

Simon, G., Chopin, C., 2001. Enstatite-sapphirine crack-related assemblages in ultrahigh-pressure pyrope megablasts, Dora–Maira massif, western Alps. Contrib. Mineral. Petrol. 140, 422–440.
Singh, J., Johannes, W., 1996. Dehydration melting of tonalites. Part II. Composition of melts and solids. Contrib. Mineral. Petrol. 125, 26–44.
Smithson, S.B., 1978. Modeling continental crust; structural and chemical constraints. Geophys. Res. Lett. 5 (9), 749–752.
Solar, G.S., Brown, M., 2001. Petrogenesis of migmatites in Maine, USA; possible source of peraluminous leucogranite in plutons? J. Petrol. 42 (4), 789–823.
Spandler, C., Yaxley, G., Green, D.H., Scott, D., 2010. Experimental phase and melting relations of metapelite in the upper mantle; implications for the petrogenesis of intraplate magmas. Contrib. Mineral. Petrol. 160 (4), 569–589.
Svenningsen, O., 2001. Onset of seafloor spreading in the Iapetus Ocean at 608 Ma: precise age of the Sarek Dyke Swarm, northern Swedish Caledonides. Precambrian Res. 110, 241–254.
Syracuse, E.M., van Keken, P.E., Abers, G.A., 2010. The global range of subduction zone thermal models. Phys. Earth & Planet. Inter. 183 (1–2), 73–90.
Taylor, S.R., McLennan, S.M.S.M., 1985. The Continental Crust; Its Composition and Evolution. Blackwell Scientific Publications, Oxford.
Thompson, J.B., Hovis, G.L., 1979. Entropy of mixing in sanidine. Am. Mineral. 64, 57–65.
Valley, P.M., Whitney, D.L., Paterson, S.R., Miller, R.B., Alsleben, H., 2003. Metamorphism of the deepest exposed arc rocks in the Cretaceous to Paleogene Cascades Belt, Washington; evidence for large-scale vertical motion in a continental arc. J. Metamorph. Geol. 21 (2), 203–220.
Vielzeuf, D., Holloway, J.R., 1988. Experimental determination of the fluid-absent melting relations in the pelitic system. Consequences for crustal differentiation. Contrib. Mineral. Petrol. 98, 257–276.
Vielzeuf, D., Montel, J.M., 1994. Partial melting of metagreywackes. 1. Fluid-absent experiments and phase relationships. Contrib. Mineral. Petrol. 117, 375–393.
von Huene, R., Scholl, D.W., 1991. Observations at convergent margins concerning sediment subduction, subduction erosion, and the growth of continental crust. Rev. Geophys. 29, 279–316.
Walsh, E.O., Hacker, B.R., 2004. The fate of subducted continental margins: two-stage exhumation of the high-pressure to ultrahigh-pressure Western Gneiss complex, Norway. J. Metamorph. Geol. 22, 671–689.
Warren, C.J., Beaumont, C., Jamieson, R.A., 2008. Modelling tectonic styles and ultra-high pressure (UHP) rock exhumation during the transition from oceanic subduction to continental collision. Earth & Planet. Sci. Lett. 267 (1–2), 129–145.
Watt, G.R., Harley, S.L., 1993. Accessory phase controls on the geochemistry of crustal melts and restites produced during water-undersaturated partial melting. Contrib. Mineral. Petrol. 114, 550–566.
Wei, C., Powell, R., 2003. Phase relations in high-pressure metapelites in the system KFMASH (K2O–FeO–MgO–Al2O3–SiO2–H2O) with application to natural rocks. Contrib. Mineral. Petrol. 145, 301–315.
Whetten, J.T., Kelley, J.C., Hanson, L.G., 1969. Characteristics of Columbia river sediment and sediment transport. J. Sediment. Petrol. 39 (3), 1149–1166.
White, R.W., Powell, R., Phillips, G.N., 2003. A mineral equilibria study of the hydrothermal alteration in mafic greenschist facies rocks at Kalgoorlie, Western Australia. J. Metamorph. Geol. 21, 455–468.
Wolf, M.B., Wyllie, P.J., 1993. Garnet growth during amphibolite anatexis: implications of a garnetiferous restite. J. Geol. 101, 357–373.
Workman, R.K., Hart, S.R., 2005. Major and trace element composition of the depleted MORB mantle (DMM). Earth & Planet. Sci. Lett. 231 (53–72).
Yamamoto, S., Senshu, H., Rino, S., Omori, S., Maruyama, S., 2009. Granite subduction: arc subduction, tectonic erosion and sediment subduction. Gondwana Res. 15, 443–453.
Yin, A., Manning, C.E., Lovera, O., Menold, C.A., Chen, X., Gehrels, G.E., 2007. Early Paleozoic tectonic and thermomechanical evolution of ultrahigh-pressure (UHP) metamorphic rocks in the northern Tibetan Plateau, northwest China. Int. Geol. Rev. 49, 681–716.
Zhang, R.Y., Liou, J.G., Ernst, W.G., Coleman, R.G., Sobolev, N.V., Shatsky, V.S., 1997. Metamorphic evolution of diamond-bearing and associated rocks from the Kokchetav massif, northern Kazakhstan. J. Metamorph. Geol. 15, 479–496.
Zhu, G., Gerya, T.V., Yuen, D.A., Honda, S., Yoshida, T., Connolly, J.A.D., 2009. Three-dimensional dynamics of hydrous thermal–chemical plumes in oceanic subduction zones. Geochem. Geophys. Geosyst. G 10 (11).